

Scaling Up Sparse Support Vector Machines by Simultaneous Feature and Sample Reduction

Weizhong Zhang^{1,2,*}, Bin Hong^{1,3,*}

Wei Liu², Jieping Ye^{3,4}, Deng Cai¹, Xiaofei He¹, Jie Wang³

¹State Key Lab of CAD&CG, College of Computer Science, Zhejiang University

²Tencent AI Lab, Shenzhen, China

³Department of Computational Medicine and Bioinformatics, University of Michigan

⁴Department of Electrical Engineering and Computer Science, University of Michigan

October 11, 2024

Abstract

Sparse support vector machine (SVM) is a popular classification technique that can simultaneously learn a small set of the most interpretable features and identify the support vectors. It has achieved great successes in many real-world applications. However, for large-scale problems involving a huge number of samples and extremely high-dimensional features, solving sparse SVMs remains challenging. By noting that sparse SVMs induce sparsities in both feature and sample spaces, we propose a novel approach, which is based on accurate estimations of the primal and dual optima of sparse SVMs, to simultaneously identify the features and samples that are guaranteed to be irrelevant to the outputs. Thus, we can remove the identified inactive samples and features from the training phase, leading to substantial savings in both the memory usage and computational cost without sacrificing accuracy. To the best of our knowledge, the proposed method is the *first static* feature and sample reduction method for sparse SVM. Experiments on both synthetic and real datasets (e.g., the kddb dataset with about 20 million samples and 30 million features) demonstrate that our approach significantly outperforms state-of-the-art methods and the speedup gained by our approach can be orders of magnitude.

1 Introduction

Sparse support vector machine (SVM) [1, 22] is a powerful technique that can simultaneously perform classification by margin maximization and variable selection by ℓ_1 -norm penalty. The last few years have witnessed many successful applications of sparse SVMs, such as text mining [10, 24], bioinformatics [13] and image processing [12, 11]. Many algorithms [7, 6, 3, 9, 16] have been proposed to efficiently solve sparse SVM problems. However, the applications of sparse SVMs to large-scale learning problems, which involve a huge number of samples and extremely high-dimensional features, remain challenging.

An emerging technique, called *screening* [5], has been shown to be promising in accelerating large-scale sparse learning. The essential idea of screening is to quickly identify the zero coefficients in the sparse solutions without solving any optimization problems such that the corresponding features or samples—that are called *inactive* features or samples—can be removed from the training phase. Then, we only need to perform optimization on the reduced datasets instead of the full datasets, leading to substantial savings in the computational cost and memory usage. Here, we need to emphasize that screening differs greatly from feature selection methods, although they look similar at the first glance. To be precise, screening

is devoted to accelerating the training of many sparse models including Lasso, Sparse SVM, etc., while feature selection is the goal of these models. In the past few years, many screening methods are proposed for a large set of sparse learning techniques, such as Lasso [19, 23, 21], group Lasso [14], ℓ_1 -regularized logistic regression [20], and SVM [15]. Empirical studies indicate that screening methods can lead to orders of magnitude of speedup in computation time.

However, most existing screening methods study either feature screening or sample screening individually [18] and their applications have very different scenarios. Specifically, to achieve better performance (say, in terms of speedup), we favor feature screening methods when the number of features p is much larger than the number of samples n , while sample screening methods are preferable when $n \gg p$. Note that there is another class of sparse learning techniques, like sparse SVMs, which induce sparsities in both feature and sample spaces. All these screening methods are helpless in accelerating the training of these models with large n and p . We also cannot address this problem by simply combining the existing feature and sample screening methods. The reason is that they could mistakenly discard relevant data as they are specifically designed for different sparse models. Recently, Shibagaki et al. [18] consider this problem and propose a method to simultaneously identify the inactive features and samples in a *dynamic* manner [2]; that is, during the optimization process, they trigger their testing rule when there is a sufficient decrease in the duality gap. Thus, the method in [18] can discard more inactive features and samples as the optimization proceeds and one has small-scale problems to solve in the late stage of the optimization. Nevertheless, the overall speedup can be limited as the problems' size can be large in the early stage of the optimization. To be specific, the method in [18] depends heavily on the duality gap during the optimization process. The duality gap in the early stage can always be large, which makes the dual and primal estimations inaccurate and finally results in ineffective screening rules. Hence, it is essentially solving a large problem in the early stage.

In this paper, to address the limitations in the dynamic screening method, we propose a novel screening method that can **S**imultaneously identify **I**nactive **F**eatures and **S**amples (SIFS) for sparse SVMs in a *static* manner, that is, we only need to perform SIFS once *before* (instead of during) optimization. Thus, we only need to run the optimization algorithm on small-scale problems. The major technical challenge in developing SIFS is that we need to accurately estimate the primal and dual optima. The more accurate the estimations are, the more effective SIFS is in detecting inactive features and samples. Thus, our major technical contribution is a novel framework, which is based on the strong convexity of the primal and dual problems of sparse SVMs [see problems (P*) and (D*) in Section 2] for deriving accurate estimations of the primal and dual optima (see Section 3). Another appealing feature of SIFS is the so-called *synergy effect* [18]. Specifically, the proposed SIFS consists of two parts, i.e., **I**nactive **F**eature **S**creening (IFS) and **I**nactive **S**amples **S**creening (ISS). We show that discarding inactive features (samples) identified by IFS (ISS) leads to a more accurate estimation of the primal (dual) optimum, which in turn dramatically enhances the capability of ISS (IFS) in detecting inactive samples (features). Thus, SIFS applies IFS and ISS in an alternating manner until no more inactive features and samples can be identified, leading to much better performance in scaling up large-scale problems than the application of ISS or IFS individually. Moreover, SIFS (see Section 4) is safe in the sense that the detected features and samples are guaranteed to be absent from the sparse representations. To the best of our knowledge, SIFS is the first static screening rule for sparse SVM that is able to simultaneously detect inactive features and samples. Experiments (see Section 5) on both synthetic and real datasets demonstrate that SIFS significantly outperforms the state-of-the-art [18] in improving the efficiency of sparse SVMs and the speedup can be orders of magnitude. Detailed proofs of theoretical results in the main text are in the supplementary supplements.

Notations: Let $\|\cdot\|_1$, $\|\cdot\|$, and $\|\cdot\|_\infty$ be the ℓ_1 , ℓ_2 , and ℓ_∞ norms, respectively. We denote the inner product of vectors \mathbf{x} and \mathbf{y} by $\langle \mathbf{x}, \mathbf{y} \rangle$, and the i -th component of \mathbf{x} by $[\mathbf{x}]_i$. Let $[p] = \{1, 2, \dots, p\}$ for a positive integer p . Given a subset $\mathcal{J} := \{j_1, \dots, j_k\}$ of $[p]$, let $|\mathcal{J}|$ be the cardinality of \mathcal{J} . For a vector \mathbf{x} , let $[\mathbf{x}]_{\mathcal{J}} = ([\mathbf{x}]_{j_1}, \dots, [\mathbf{x}]_{j_k})^T$. For a matrix \mathbf{X} , let $[\mathbf{X}]_{\mathcal{J}} = (\mathbf{x}_{j_1}, \dots, \mathbf{x}_{j_k})$ and $_{\mathcal{J}}[\mathbf{X}] = ((\mathbf{x}^{j_1})^T, \dots, (\mathbf{x}^{j_k})^T)^T$, where \mathbf{x}^i and \mathbf{x}_j are the i^{th} row and j^{th} column of \mathbf{X} , respectively. For a scalar t , we denote $\max\{0, t\}$ by $[t]_+$.

2 Basics and Motivations

In this section, we briefly review some basics of sparse SVMs and then motivate SIFS via the KKT conditions. Specifically, we focus on the ℓ_1 -regularized SVM with a smoothed hinged loss that has strong theoretical guarantees [17], which takes the form of

$$\min_{\mathbf{w} \in \mathbb{R}^p} P(\mathbf{w}; \alpha, \beta) = \frac{1}{n} \sum_{i=1}^n \ell(1 - \langle \bar{\mathbf{x}}_i, \mathbf{w} \rangle) + \frac{\alpha}{2} \|\mathbf{w}\|^2 + \beta \|\mathbf{w}\|_1, \quad (\text{P}^*)$$

where \mathbf{w} is the parameter vector to be estimated, $\{\mathbf{x}_i, y_i\}_{i=1}^n$ is the training set, $\mathbf{x}_i \in \mathbb{R}^p$, $y_i \in \{-1, +1\}$, $\bar{\mathbf{x}}_i = y_i \mathbf{x}_i$, α and β are positive parameters, and the loss function $\ell(\cdot) : \mathbb{R} \rightarrow \mathbb{R}$ is

$$\ell(t) = \begin{cases} 0, & \text{if } t < 0, \\ \frac{t^2}{2\gamma}, & \text{if } 0 \leq t \leq \gamma, \\ t - \frac{\gamma}{2}, & \text{if } t > \gamma, \end{cases}$$

where $\gamma \in (0, 1)$. We present the Lagrangian dual problem of problem (P*) and the KKT conditions in the following theorem, which plays a fundamentally important role in developing our screening rule.

Theorem 1. Let $\bar{\mathbf{X}} = (\bar{\mathbf{x}}_1, \bar{\mathbf{x}}_2, \dots, \bar{\mathbf{x}}_n)$ and $\mathcal{S}_\beta(\cdot)$ be the soft-thresholding operator [8], i.e., $[\mathcal{S}_\beta(\mathbf{u})]_i = \text{sign}([\mathbf{u}]_i)(|[\mathbf{u}]_i| - \beta)_+$. Then, for problem (P*), the followings hold:

(i) : The dual problem of (P*) is

$$\min_{\theta \in [0, 1]^n} D(\theta; \alpha, \beta) = \frac{1}{2\alpha} \left\| \mathcal{S}_\beta \left(\frac{1}{n} \bar{\mathbf{X}} \theta \right) \right\|^2 + \frac{\gamma}{2n} \|\theta\|^2 - \frac{1}{n} \langle \mathbf{1}, \theta \rangle, \quad (\text{D}^*)$$

where $\mathbf{1} \in \mathbb{R}^n$ is a vector with all components equal to 1.

(ii) : Denote the optima of (P*) and (D*) by $\mathbf{w}^*(\alpha, \beta)$ and $\theta^*(\alpha, \beta)$, respectively. Then,

$$\mathbf{w}^*(\alpha, \beta) = \frac{1}{\alpha} \mathcal{S}_\beta \left(\frac{1}{n} \bar{\mathbf{X}} \theta^*(\alpha, \beta) \right), \quad (\text{KKT-1})$$

$$[\theta^*(\alpha, \beta)]_i = \begin{cases} 0, & \text{if } 1 - \langle \bar{\mathbf{x}}_i, \mathbf{w}^*(\alpha, \beta) \rangle < 0; \\ 1, & \text{if } 1 - \langle \bar{\mathbf{x}}_i, \mathbf{w}^*(\alpha, \beta) \rangle > \gamma; \\ \frac{1}{\gamma} (1 - \langle \bar{\mathbf{x}}_i, \mathbf{w}^*(\alpha, \beta) \rangle), & \text{otherwise.} \end{cases} \quad (\text{KKT-2})$$

According to KKT-1 and KKT-2, we define 4 index sets:

$$\begin{aligned} \mathcal{F} &= \left\{ j \in [p] : \frac{1}{n} |[\bar{\mathbf{X}} \theta^*(\alpha, \beta)]_j| \leq \beta \right\}, \\ \mathcal{R} &= \{i \in [n] : 1 - \langle \mathbf{w}^*(\alpha, \beta), \bar{\mathbf{x}}_i \rangle < 0\}, \\ \mathcal{E} &= \{i \in [n] : 1 - \langle \mathbf{w}^*(\alpha, \beta), \bar{\mathbf{x}}_i \rangle \in [0, \gamma]\}, \\ \mathcal{L} &= \{i \in [n] : 1 - \langle \mathbf{w}^*(\alpha, \beta), \bar{\mathbf{x}}_i \rangle > \gamma\}, \end{aligned}$$

which imply that

$$(i): i \in \mathcal{F} \Rightarrow [\mathbf{w}^*(\alpha, \beta)]_i = 0, (ii): \begin{cases} i \in \mathcal{R} \Rightarrow [\theta^*(\alpha, \beta)]_i = 0, \\ i \in \mathcal{L} \Rightarrow [\theta^*(\alpha, \beta)]_i = 1. \end{cases} \quad (\text{R})$$

Thus, we call the j^{th} feature *inactive* if $j \in \mathcal{F}$. The samples in \mathcal{E} are the so-called support vectors and we call the samples in \mathcal{R} and \mathcal{L} *inactive* samples.

Suppose that we are given subsets of \mathcal{F} , \mathcal{R} , and \mathcal{L} , then by (R), we can see that many coefficients of $\mathbf{w}^*(\alpha, \beta)$ and $\theta^*(\alpha, \beta)$ are known. Thus, we may have much less unknowns to solve and the problem size can be dramatically reduced. We formalize this idea in Lemma 1.

Lemma 1. *Given index sets $\hat{\mathcal{F}} \subseteq \mathcal{F}$, $\hat{\mathcal{R}} \subseteq \mathcal{R}$, and $\hat{\mathcal{L}} \subseteq \mathcal{L}$, the followings hold*

- (i) : $[\mathbf{w}^*(\alpha, \beta)]_{\hat{\mathcal{F}}} = 0$, $[\theta^*(\alpha, \beta)]_{\hat{\mathcal{R}}} = 0$, $[\theta^*(\alpha, \beta)]_{\hat{\mathcal{L}}} = 1$.
(ii) : Let $\hat{\mathcal{D}} = \hat{\mathcal{R}} \cup \hat{\mathcal{L}}$, $\hat{\mathbf{G}}_1 = \frac{1}{|\hat{\mathcal{D}}^c|} [\bar{\mathbf{X}}]_{\hat{\mathcal{D}}^c}$, and $\hat{\mathbf{G}}_2 = \frac{1}{|\hat{\mathcal{L}}|} [\bar{\mathbf{X}}]_{\hat{\mathcal{L}}}$, where $\hat{\mathcal{F}}^c = [p] \setminus \hat{\mathcal{F}}$, $\hat{\mathcal{D}}^c = [n] \setminus \hat{\mathcal{D}}$, and $\hat{\mathcal{L}}^c = [n] \setminus \hat{\mathcal{L}}$. Then, $[\theta^*(\alpha, \beta)]_{\hat{\mathcal{D}}^c}$ solves the following scaled dual problem:

$$\min_{\hat{\theta} \in [0, 1]^{|\hat{\mathcal{D}}^c|}} \left\{ \frac{1}{2\alpha} \left\| \mathcal{S}_\beta \left(\frac{1}{n} \hat{\mathbf{G}}_1 \hat{\theta} + \frac{1}{n} \hat{\mathbf{G}}_2 \mathbf{1} \right) \right\|^2 + \frac{\gamma}{2n} \|\hat{\theta}\|^2 - \frac{1}{n} \langle \mathbf{1}, \hat{\theta} \rangle \right\}. \quad (\text{scaled-D}^*)$$

- (iii) : Suppose that $\theta^*(\alpha, \beta)$ is known. Then,

$$[\mathbf{w}^*(\alpha, \beta)]_{\hat{\mathcal{F}}^c} = \frac{1}{\alpha} \mathcal{S}_\beta \left(\frac{1}{n} [\bar{\mathbf{X}}]_{\hat{\mathcal{F}}^c} \theta^*(\alpha, \beta) \right).$$

Lemma 1 indicates that, if we can identify index sets $\hat{\mathcal{F}}$ and $\hat{\mathcal{D}}$ and the cardinalities of $\hat{\mathcal{F}}^c$ and $\hat{\mathcal{D}}^c$ are much smaller than the feature dimension p and the dataset size n , we only need to solve a problem (scaled-D*) that may be much *smaller* than problem (D*) to exactly recover the optima $\mathbf{w}^*(\alpha, \beta)$ and $\theta^*(\alpha, \beta)$ *without sacrificing any accuracy*.

However, we cannot directly apply the rules in (R) to identify subsets of \mathcal{F} , \mathcal{R} , and \mathcal{L} , as they require the knowledge of $\mathbf{w}^*(\alpha, \beta)$ and $\theta^*(\alpha, \beta)$ that are usually unavailable. Inspired by the idea in [5], we can first estimate regions \mathcal{W} and Θ that contain $\mathbf{w}^*(\alpha, \beta)$ and $\theta^*(\alpha, \beta)$, respectively. Then, by denoting

$$\hat{\mathcal{F}} := \left\{ j \in [p] : \max_{\theta \in \Theta} \left\{ \left| \frac{1}{n} [\bar{\mathbf{X}} \theta]_j \right| \right\} \leq \beta \right\}, \quad (1)$$

$$\hat{\mathcal{R}} := \left\{ i \in [n] : \max_{\mathbf{w} \in \mathcal{W}} \{1 - \langle \mathbf{w}, \bar{\mathbf{x}}_i \rangle\} < 0 \right\}, \quad (2)$$

$$\hat{\mathcal{L}} := \left\{ i \in [n] : \min_{\mathbf{w} \in \mathcal{W}} \{1 - \langle \mathbf{w}, \bar{\mathbf{x}}_i \rangle\} > \gamma \right\}, \quad (3)$$

since it is easy to know that $\hat{\mathcal{F}} \subseteq \mathcal{F}$, $\hat{\mathcal{R}} \subseteq \mathcal{R}$ and $\hat{\mathcal{L}} \subseteq \mathcal{L}$, the rules in (R) can be relaxed as follows:

$$(i): j \in \hat{\mathcal{F}} \Rightarrow [\mathbf{w}^*(\alpha, \beta)]_j = 0, \quad (\text{R1})$$

$$(ii): \begin{cases} i \in \hat{\mathcal{R}} \Rightarrow [\theta^*(\alpha, \beta)]_i = 0, \\ i \in \hat{\mathcal{L}} \Rightarrow [\theta^*(\alpha, \beta)]_i = 1. \end{cases} \quad (\text{R2})$$

In view of R1 and R2, we sketch the development of SIFS as follows.

Step 1: Derive estimations \mathcal{W} and Θ such that $\mathbf{w}^*(\alpha, \beta) \in \mathcal{W}$ and $\theta^*(\alpha, \beta) \in \Theta$, respectively.

Step 2: Develop SIFS by deriving the relaxed screening rules R1 and R2, i.e., by solving the optimization problems in Eq. (1), Eq. (2) and Eq. (3).

3 Estimate the Primal and Dual Optima

In this section, we first show that the primal and dual optima admit closed form solutions for specific values of α and β (see Section 3.1). Then, in Sections 3.2 and 3.3, we present accurate estimations of the primal and dual optima, respectively.

3.1 Effective Intervals of the Parameters α and β

We first show that, if the value of β is sufficiently large, no matter what α is, the primal solution is 0.

Theorem 2. *Let $\beta_{\max} = \|\frac{1}{n}\bar{\mathbf{X}}\mathbf{1}\|_{\infty}$. Then, for $\alpha > 0$ and $\beta \geq \beta_{\max}$, we have*

$$\mathbf{w}^*(\alpha, \beta) = \mathbf{0}, \quad \theta^*(\alpha, \beta) = \mathbf{1}.$$

For any β , the next result shows that, if α is large enough, the primal and dual optima admit closed form solutions.

Theorem 3. *If we denote*

$$\alpha_{\max}(\beta) = \frac{1}{1-\gamma} \max_{i \in [n]} \{ \langle \bar{\mathbf{x}}_i, \mathcal{S}_{\beta}(\frac{1}{n}\bar{\mathbf{X}}\mathbf{1}) \rangle \},$$

then for all $\alpha \in [\max\{\alpha_{\max}(\beta), 0\}, \infty) \cap (0, \infty)$, we have

$$\mathbf{w}^*(\alpha, \beta) = \frac{1}{\alpha} \mathcal{S}_{\beta} \left(\frac{1}{n} \bar{\mathbf{X}} \mathbf{1} \right), \quad \theta^*(\alpha, \beta) = \mathbf{1}. \quad (4)$$

By Theorems 2 and 3, we only need to consider the cases with $\beta \in (0, \beta_{\max}]$ and $\alpha \in (0, \alpha_{\max}(\beta)]$.

3.2 Primal Optimum Estimation

In Section 1, we mention that the proposed SIFS consists of IFS and ISS, and an alternating application of IFS and ISS can improve the estimation of the primal and dual optima, which can in turn make ISS and IFS more effective in identifying inactive samples and features, respectively. Lemma 2 shows that discarding inactive features by IFS leads to a more accurate estimation of the primal optimum.

Lemma 2. *Suppose that the reference solution $\mathbf{w}^*(\alpha_0, \beta_0)$ with $\beta_0 \in (0, \beta_{\max}]$ and $\alpha_0 \in (0, \alpha_{\max}(\beta_0)]$ is known. Consider problem (P*) with parameters $\alpha > 0$ and β_0 . Let $\hat{\mathcal{F}}$ be the index set of the inactive features identified by the previous IFS steps, i.e., $[\mathbf{w}^*(\alpha, \beta_0)]_{\hat{\mathcal{F}}} = \mathbf{0}$. We define*

$$\mathbf{c} = \frac{\alpha_0 + \alpha}{2\alpha} [\mathbf{w}^*(\alpha_0, \beta_0)]_{\hat{\mathcal{F}}^c}, \quad (5)$$

$$r^2 = \frac{(\alpha_0 - \alpha)^2}{4\alpha^2} \|\mathbf{w}^*(\alpha_0, \beta_0)\|^2 - \frac{(\alpha_0 + \alpha)^2}{4\alpha^2} \|[\mathbf{w}^*(\alpha_0, \beta_0)]_{\hat{\mathcal{F}}}\|^2. \quad (6)$$

Then, the following holds:

$$[\mathbf{w}^*(\alpha, \beta_0)]_{\hat{\mathcal{F}}^c} \in \mathcal{W} := \{\mathbf{w} : \|\mathbf{w} - \mathbf{c}\| \leq r\}. \quad (7)$$

As $\hat{\mathcal{F}}$ is the index set of identified inactive features, we have $[\mathbf{w}^*(\alpha, \beta_0)]_{\hat{\mathcal{F}}} = \mathbf{0}$. Hence, we only need to find an accurate estimation of $[\mathbf{w}^*(\alpha, \beta_0)]_{\hat{\mathcal{F}}^c}$. Lemma 2 shows that $[\mathbf{w}^*(\alpha, \beta_0)]_{\hat{\mathcal{F}}^c}$ lies in a ball of radius r centered at \mathbf{c} . Note that, before we perform IFS, the set $\hat{\mathcal{F}}$ is empty and thus the second term on the right hand side (RHS) of Eq. (6) is 0. If we apply IFS multiple times (alternating with ISS), the set $\hat{\mathcal{F}}$ will be monotonically increasing. Thus, Eq. (6) implies that the radius will be monotonically decreasing, leading to a more accurate primal optimum estimation.

3.3 Dual Optimum Estimation

Similar to Lemma 2, the next result shows that ISS can improve the estimation of the dual optimum.

Lemma 3. *Suppose that the reference solution $\theta^*(\alpha_0, \beta_0)$ with $\beta_0 \in (0, \beta_{\max}]$ and $\alpha_0 \in (0, \alpha_{\max}(\beta_0)]$ is known. Consider problem (D*) with parameters $\alpha > 0$ and β_0 . Let $\hat{\mathcal{R}}$ and $\hat{\mathcal{L}}$ be the index sets of inactive samples identified by the previous ISS steps, i.e., $[\theta^*(\alpha, \beta_0)]_{\hat{\mathcal{R}}} = \mathbf{0}$, $[\theta^*(\alpha, \beta_0)]_{\hat{\mathcal{L}}} = \mathbf{1}$, and $\hat{\mathcal{D}} = \hat{\mathcal{R}} \cup \hat{\mathcal{L}}$. We define*

$$\mathbf{c} = \frac{\alpha - \alpha_0}{2\gamma\alpha} \mathbf{1} + \frac{\alpha_0 + \alpha}{2\alpha} [\theta^*(\alpha_0, \beta_0)]_{\hat{\mathcal{D}}^c}, \quad (8)$$

$$r^2 = \frac{(\alpha_0 - \alpha)^2}{4\alpha^2} \left\| \theta^*(\alpha_0, \beta_0) - \frac{1}{\gamma} \mathbf{1} \right\|^2 - \left\| \frac{(2\gamma - 1)\alpha + \alpha_0}{2\gamma\alpha} \mathbf{1} - \frac{\alpha_0 + \alpha}{2\alpha} [\theta^*(\alpha_0, \beta_0)]_{\hat{\mathcal{L}}} \right\|^2 - \left\| \frac{\alpha - \alpha_0}{2\gamma\alpha} \mathbf{1} + \frac{\alpha_0 + \alpha}{2\alpha} [\theta^*(\alpha_0, \beta_0)]_{\hat{\mathcal{R}}} \right\|^2. \quad (9)$$

Then, the following holds:

$$[\theta^*(\alpha, \beta_0)]_{\hat{\mathcal{D}}^c} \in \Theta := \{\theta : \theta - \mathbf{c}\| \leq r\}. \quad (10)$$

Similar to Lemma 2, Lemma 3 also bounds $[\theta^*(\alpha, \beta_0)]_{\hat{\mathcal{D}}^c}$ by a ball. In view of Eq. (9), a similar discussion of Lemma 2—that is, the index sets $\hat{\mathcal{L}}$ and $\hat{\mathcal{R}}$ monotonically increase and thus the last two terms on the RHS of Eq. (9) monotonically increase when we perform ISS multiple times (alternating with IFS)—implies that the ISS steps can reduce the radius and thus improve the dual optimum estimation.

Remark 1. *To estimate $\mathbf{w}^*(\alpha, \beta_0)$ and $\theta^*(\alpha, \beta_0)$ by Lemmas 2 and 3, we have a free reference solution pair $\mathbf{w}^*(\alpha_0, \beta_0)$ and $\theta^*(\alpha_0, \beta_0)$ with $\alpha_0 = \alpha_{\max}(\beta_0)$. From Theorems 2 and 3, we know that in this setting, $\mathbf{w}^*(\alpha_0, \beta_0)$ and $\theta^*(\alpha_0, \beta_0)$ admit closed form solutions.*

4 The Proposed SIFS Screening Rule

We first present the IFS and ISS rules in Sections 4.1 and 4.2, respectively. Then, in Section 4.3, we develop the SIFS screening rule by an alternating application of IFS and ISS.

4.1 Inactive Feature Screening (IFS)

Suppose that $\mathbf{w}^*(\alpha_0, \beta_0)$ and $\theta^*(\alpha_0, \beta_0)$ are known, we derive IFS to identify inactive features for problem (P*) at (α, β_0) by solving the optimization problem in Eq. (1) (see Section E in the supplementary material):

$$s^i(\alpha, \beta_0) = \max_{\theta \in \Theta} \left\{ \frac{1}{n} |\langle [\bar{\mathbf{x}}^i]_{\hat{\mathcal{D}}^c}, \theta \rangle + \langle [\bar{\mathbf{x}}^i]_{\hat{\mathcal{L}}}, \mathbf{1} \rangle| \right\}, i \in \hat{\mathcal{F}}^c, \quad (11)$$

where Θ is given by Eq. (10) and $\hat{\mathcal{F}}$ and $\hat{\mathcal{D}} = \hat{\mathcal{R}} \cup \hat{\mathcal{L}}$ are the index sets of inactive features and samples that have been identified in previous screening processes, respectively. The next result shows the closed form solution of problem (11).

Lemma 4. *Consider problem (11). Let \mathbf{c} and r be given by Eq. (8) and Eq. (9). Then, for all $i \in \hat{\mathcal{F}}^c$, we have*

$$s^i(\alpha, \beta_0) = \frac{1}{n} (|\langle [\bar{\mathbf{x}}^i]_{\hat{\mathcal{D}}^c}, \mathbf{c} \rangle + \langle [\bar{\mathbf{x}}^i]_{\hat{\mathcal{L}}}, \mathbf{1} \rangle| + \|[\bar{\mathbf{x}}^i]_{\hat{\mathcal{D}}^c} \| r).$$

We are now ready to present the IFS rule.

Theorem 4. *Consider problem (P*). We suppose that $\mathbf{w}^*(\alpha_0, \beta_0)$ and $\theta^*(\alpha_0, \beta_0)$ are known. Then,*

(1): *The feature screening rule IFS takes the form of*

$$s^i(\alpha, \beta_0) \leq \beta_0 \Rightarrow [\mathbf{w}^*(\alpha, \beta_0)]_i = 0, \forall i \in \hat{\mathcal{F}}^c \quad (\text{IFS})$$

(2): *We update the index set $\hat{\mathcal{F}}$ by*

$$\hat{\mathcal{F}} \leftarrow \hat{\mathcal{F}} \cup \{i : s^i \leq \beta_0, i \in \hat{\mathcal{F}}^c\}. \quad (12)$$

Recall that (Lemma 3), previous sample screening results give us a more tighter dual estimation, i.e., a smaller feasible region Θ for problem (11), which results in a smaller $s^i(\alpha, \beta_0)$. It finally leads us to a more powerful feature screening rule IFS. This is the so called synergy effect.

4.2 Inactive Sample Screening (ISS)

Similar to IFS, we derive ISS to identify inactive samples by solving the optimization problems in Eq. (2) and Eq. (3) (see Section G in the supplementary material for details):

$$u_i(\alpha, \beta_0) = \max_{\mathbf{w} \in \mathcal{W}} \{1 - \langle [\bar{\mathbf{x}}_i]_{\hat{\mathcal{F}}^c}, \mathbf{w} \rangle\}, i \in \hat{\mathcal{D}}^c, \quad (13)$$

$$l_i(\alpha, \beta_0) = \min_{\mathbf{w} \in \mathcal{W}} \{1 - \langle [\bar{\mathbf{x}}_i]_{\hat{\mathcal{F}}^c}, \mathbf{w} \rangle\}, i \in \hat{\mathcal{D}}^c, \quad (14)$$

where \mathcal{W} is given by Eq. (7) and $\hat{\mathcal{F}}$ and $\hat{\mathcal{D}} = \hat{\mathcal{R}} \cup \hat{\mathcal{L}}$ are the index sets of inactive features and samples that have been identified in previous screening processes. We show that problems (13) and (14) admit closed form solutions.

Lemma 5. *Consider problems (13) and (14). Let \mathbf{c} and r be given by Eq. (5) and Eq. (6). Then,*

$$u_i(\alpha, \beta_0) = 1 - \langle [\bar{\mathbf{x}}_i]_{\hat{\mathcal{F}}^c}, \mathbf{c} \rangle + \|[\bar{\mathbf{x}}_i]_{\hat{\mathcal{F}}^c} \| r, i \in \hat{\mathcal{D}}^c,$$

$$l_i(\alpha, \beta_0) = 1 - \langle [\bar{\mathbf{x}}_i]_{\hat{\mathcal{F}}^c}, \mathbf{c} \rangle - \|[\bar{\mathbf{x}}_i]_{\hat{\mathcal{F}}^c} \| r, i \in \hat{\mathcal{D}}^c.$$

We are now ready to present the ISS rule.

Theorem 5. *Consider problem (D*). We suppose that $\mathbf{w}^*(\alpha_0, \beta_0)$ and $\theta^*(\alpha_0, \beta_0)$ are known. Then,*

(1): *The sample screening rule ISS takes the form of*

$$\begin{aligned} u_i(\alpha, \beta_0) < 0 &\Rightarrow [\theta^*(\alpha, \beta_0)]_i = 0, \\ l_i(\alpha, \beta_0) > \gamma &\Rightarrow [\theta^*(\alpha, \beta_0)]_i = 1, \end{aligned} \quad \forall i \in \hat{\mathcal{D}}^c \quad (\text{ISS})$$

(2): *We update the the index sets $\hat{\mathcal{R}}$ and $\hat{\mathcal{L}}$ by*

$$\hat{\mathcal{R}} \leftarrow \hat{\mathcal{R}} \cup \{i : u_i(\alpha, \beta_0) < 0, i \in \hat{\mathcal{D}}^c\}, \quad (15)$$

$$\hat{\mathcal{L}} \leftarrow \hat{\mathcal{L}} \cup \{i : l_i(\alpha, \beta_0) > \gamma, i \in \hat{\mathcal{D}}^c\}. \quad (16)$$

The synergy effect also exists here. Recall that (Lemma 2), previous feature screening results lead a smaller feasible region \mathcal{W} for the problems (13) and (14), which results in smaller $u_i(\alpha, \beta_0)$ and bigger $l_i(\alpha, \beta_0)$. It finally leads us to a more accurate sample screening rule ISS.

4.3 The Proposed SIFS Rule by An Alternating Application of IFS and ISS

In real applications, the optimal parameter values of α and β are usually unknown. To determine appropriate parameter values, common approaches, like cross validation and stability selection, need to solve the model over a grid of parameter values $\{(\alpha_{i,j}, \beta_j) : i \in [M], j \in [N]\}$ with $\beta_{\max} > \beta_1 > \dots > \beta_N > 0$ and $\alpha_{\max}(\beta_j) > \alpha_{1,j} > \dots > \alpha_{M,j} > 0$. This can be very time-consuming. Inspired by Strong Rule [19] and SAFE [5], we develop a sequential version of SIFS in Algorithm 1. Specifically, given the primal and dual optima $\mathbf{w}^*(\alpha_{i-1,j}, \beta_j)$ and

Algorithm 1 SIFS

```

1: Input:  $\beta_{\max} > \beta_1 > \dots > \beta_N > 0$  and  $\alpha_{\max}(\beta_j) = \alpha_{0,j} > \alpha_{1,j} > \dots > \alpha_{M,j} > 0$ .
2: for  $j = 1$  to  $N$  do
3:   Compute the first reference solution  $\mathbf{w}^*(\alpha_{0,j}, \beta_j)$  and  $\theta^*(\alpha_{0,j}, \beta_j)$  using the close-form formula (4).
4:   for  $i = 1$  to  $M$  do
5:     Initialization:  $\hat{\mathcal{F}} = \hat{\mathcal{R}} = \hat{\mathcal{L}} = \emptyset$ 
6:     repeat
7:       Run sample screening using rule ISS based on  $\mathbf{w}^*(\alpha_{i-1,j}, \beta_j)$ .
8:       Update  $\hat{\mathcal{R}}$  and  $\hat{\mathcal{L}}$  by Eq. (15) and Eq. (16), respectively.
9:       Run feature screening using rule IFS based on  $\theta^*(\alpha_{i-1,j}, \beta_j)$ .
10:      Update  $\hat{\mathcal{F}}$  by Eq. (12).
11:     until No new inactive features or samples are identified
12:     Compute  $\mathbf{w}^*(\alpha_{i,j}, \beta_j)$  and  $\theta^*(\alpha_{i,j}, \beta_j)$  by solving the scaled problem.
13:   end for
14: end for
15: Output:  $\mathbf{w}^*(\alpha_{i,j}, \beta_j)$  and  $\theta^*(\alpha_{i,j}, \beta_j), i \in [M], j \in [N]$ .

```

$\theta^*(\alpha_{i-1,j}, \beta_j)$ at $(\alpha_{i-1,j}, \beta_j)$, we apply SIFS to identify the inactive features and samples for problem (P*) at $(\alpha_{i,j}, \beta_j)$. Then, we perform optimization on the reduced dataset and solve the primal and dual optima at $(\alpha_{i,j}, \beta_j)$. We repeat this process until we solve problem (P*) at all pairs of parameter values.

Note that we insert $\alpha_{0,j}$ into every sequence $\{\alpha_{i,j} : i \in [M]\}$ (see line 1 in Algorithm 1) to obtain a closed-form solution as the first reference solution. In this way, we can avoid solving problem at $(\alpha_{1,j}, \beta_j), j \in [N]$ directly (without screening), which is time consuming. At last, we would like to point out that the values $\{(\alpha_{i,j}, \beta_j) : i \in [M], j \in [N]\}$ in SIFS can be specified by users arbitrarily.

SIFS applies ISS and IFS in an alternating manner to reinforce their capability in identifying inactive samples and features. In Algorithm 1, we apply ISS first. Of course, we can also apply IFS first. The theorem below demonstrates that the orders have no impact on the performance of SIFS.

Theorem 6. *Given the optimal solutions $\mathbf{w}^*(\alpha_{i-1,j}, \beta_j)$ and $\theta^*(\alpha_{i-1,j}, \beta_j)$ at $(\alpha_{i-1,j}, \beta_j)$ as the reference solution pair at $(\alpha_{i,j}, \beta_j)$ for SIFS, we assume SIFS with ISS first stops after applying IFS and ISS for p times and denote the identified inactive features and samples as $\hat{\mathcal{F}}_p^A, \hat{\mathcal{R}}_p^A$ and $\hat{\mathcal{L}}_p^A$. Similarly, when we apply IFS first, the results are denoted as $\hat{\mathcal{F}}_q^B, \hat{\mathcal{R}}_q^B$ and $\hat{\mathcal{L}}_q^B$. Then, the followings hold:*

- (1) $\hat{\mathcal{F}}_p^A = \hat{\mathcal{F}}_q^B, \hat{\mathcal{R}}_p^A = \hat{\mathcal{R}}_q^B$ and $\hat{\mathcal{L}}_p^A = \hat{\mathcal{L}}_q^B$.
- (2) With different orders of applying ISS and IFS, the difference of the times of ISS and IFS we need to apply in SIFS can never be larger than 1, that is, $|p - q| \leq 1$.

Remark 2. From Remark 1, we can see that our SIFS can also be applied to solve a single problem, due to the existence of the free reference solution pair.

5 Experiments

We evaluate SIFS on both synthetic and real datasets in terms of three measurements. The first one is the *scaling ratio*: $1 - \frac{(n-\tilde{n})(p-\tilde{p})}{np}$, where \tilde{n} , \tilde{p} , n , and p are the numbers of inactive samples and features identified by SIFS, sample size, and feature dimension of the datasets. The second measure is *rejection ratios* of each triggering of ISS and IFS in SIFS: $\frac{\tilde{n}_i}{n_0}$ and $\frac{\tilde{p}_i}{p_0}$, where \tilde{n}^i and \tilde{p}^i are the numbers of inactive samples and features identified in i -th triggering of ISS and IFS in SIFS. n_0 and p_0 are the numbers of inactive samples and features in the solution. The third measure is *speedup*, i.e., the ratio of the running time of the solver without screening to that with screening.

Recall that, we can integrate SIFS with any solvers for problem (P*). In this experiment, we use Accelerated Proximal Stochastic Dual Coordinate Ascent (Accelerated-Prox-SDCA) [17], as it is one of the state-of-the-arts. As we mentioned in the introduction section that screening differs greatly from features selection methods, it is not appropriate to make comparisons with feature selection methods. To this end, we only choose the state-of-art screening method for Sparse SVMs in [18] as a baseline in the experiments.

For each dataset, we solve problem (P*) at a grid of turning parameter values. Specifically, we first compute β_{\max} by Theorem 2 and then select 10 values of β that are equally spaced on the logarithmic scale of β/β_{\max} from 1 to 0.05. Then, for each value of β , we first compute $\alpha_{\max}(\beta)$ by Theorem 3 and then select 100 values of α that are equally spaced on the logarithmic scale of $\alpha/\alpha_{\max}(\beta)$ from 1 to 0.01. Thus, for each dataset, we solve problem (P*) at 1000 pairs of parameter values in total. We write the code in C++ along with Eigen library for some numerical computations. We perform all the computations on a single core of Intel(R) Core(TM) i7-5930K 3.50GHz, 128GB MEM.

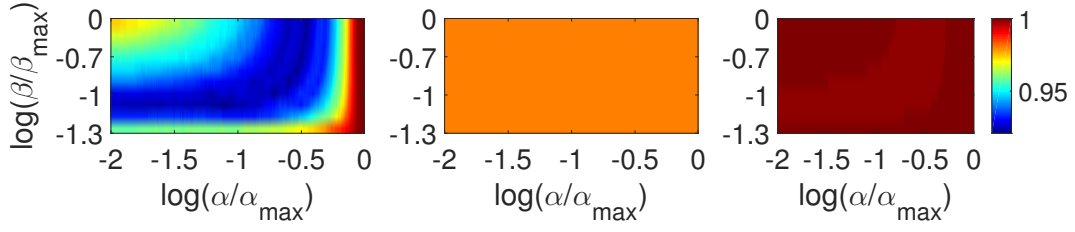
5.1 Simulation Studies

We evaluate SIFS on 3 synthetic datasets named syn1, syn2 and syn3 with sample and feature size $(n, p) \in \{(10000, 1000), (10000, 10000), (1000, 10000)\}$. We present each data point as $\mathbf{x} = [\mathbf{x}_1; \mathbf{x}_2]$ with $\mathbf{x}_1 \in \mathbb{R}^{0.02p}$ and $\mathbf{x}_2 \in \mathbb{R}^{0.98p}$. We use Gaussian distributions $\mathcal{G}_1 = N(\mathbf{u}, 0.75\mathbf{I})$, $\mathcal{G}_2 = N(-\mathbf{u}, 0.75\mathbf{I})$ and $\mathcal{G}_3 = N(0, 1)$ to generate the data points, where $\mathbf{u} = 1.5\mathbf{1}$ and $\mathbf{I} \in \mathbb{R}^{0.02p \times 0.02p}$ is the identity matrix. To be precise, \mathbf{x}_1 for positive and negative points are sampled from \mathcal{G}_1 and \mathcal{G}_2 , respectively. For each entry in \mathbf{x}_2 , it has chance $\eta = 0.02$ to be sampled from \mathcal{G}_3 and chance $1 - \eta$ to be 0.

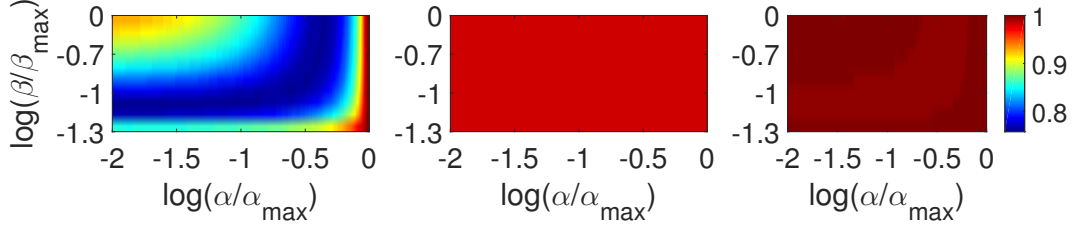
Fig. 1 shows the scaling ratios by ISS, IFS, and SIFS on the synthetic datasets at 1000 parameter values. We can see that IFS is more effective in scaling problem size than ISS, with scaling ratios roughly 98% against 70 – 90%. Moreover, SIFS, which is an alternating application of IFS and ISS, significantly outperforms ISS and IFS, with scaling ratios roughly 99.9%. This high scaling ratios imply that SIFS can lead to a significant speedup.

Table 1: Running time (in seconds) for solving problem (P*) at 1000 pairs of parameter values on three synthetic datasets.

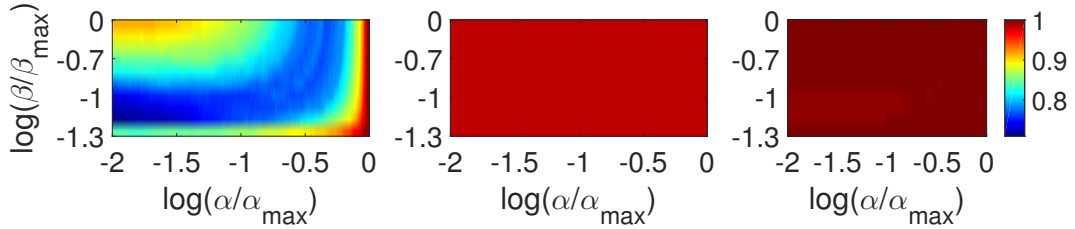
Data	Solver	ISS+Solver			IFS+Solver			SIFS+Solver		
		ISS	Solver	Speedup	IFS	Solver	Speedup	SIFS	Solver	Speedup
syn1	499.1	4.9	27.8	15.3	2.3	42.6	11.1	8.6	6.0	34.2
syn2	8749.9	24.9	1496.6	5.8	23.0	288.1	28.1	92.6	70.3	53.7
syn3	1279.7	2.0	257.1	4.9	2.2	33.4	36.0	7.2	9.5	76.8



(a) The scaling ratios of ISS, IFS, and SIFS on syn1.



(b) The scaling ratios of ISS, IFS, and SIFS on syn2.



(c) The scaling ratios of ISS, IFS, and SIFS on syn3.

Figure 1: Scaling ratios of ISS, IFS and SIFS (from left to right).

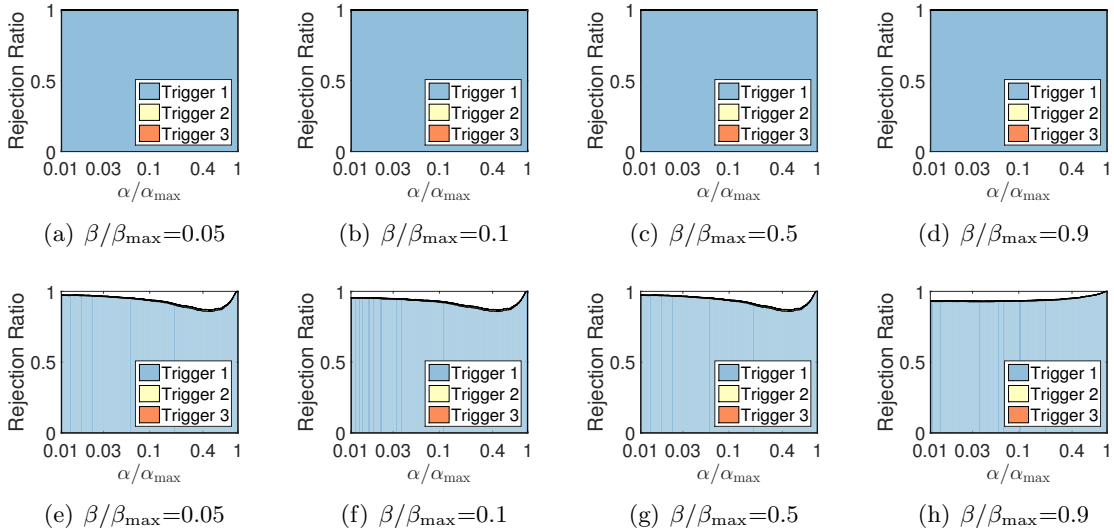


Figure 2: Rejection ratios of SIFS on syn 2 (first row: Feature Screening, second row: Sample Screening).

Due to the space limitation, we only report the rejection ratios of SIFS on syn2. Other results can be found in the supplementary material. Fig. 2 shows that SIFS can identify most of the inactive features and samples. However, few features and samples are identified in the

second and later triggerings of ISS and IFS. The reason may be that the task here is so simple that one triggering is enough.

Table 1 reports the running time of solver without and with IFS, ISS and SIFS for solving problem (P*) at 1000 pairs of parameter values. We can see that SIFS leads to significant speedups, that is, up to 76.8 times. Taking syn2 for example, without SIFS, the solver takes more than two hours to solve problem (P*) at 1000 pairs of parameter values. However, combined with SIFS, the solver only needs less than three minutes for solving the same set of problems. From the theoretical analysis in [17] for Accelerated-Prox-SDCA, we can see that its computational complexity rises proportionately to the sample size n and the feature dimension p . From this theoretical result, we can see that the results in Figure 1 are roughly consistent with the speedups we achieved shown in Table 1.

5.2 Experiments on Real Datasets

In this experiment, we evaluate the performance of SIFS on 5 large-scale real datasets: real-sim, rcv1-train, rcv1-test, url, and kddb, which are all collected from the project page of LibSVM [4]. See Table 2 for a brief summary. We note that, the kddb dataset has about 20 million samples with 30 million features.

Table 2: Statistics of the real datasets.

Dataset	Feature size: p	Sample size: n
real-sim	20,958	72,309
rcv1-train	47,236	20,242
rcv1-test	47,236	677, 399
url	3,231,961	2,396,130
kddb	29,890,095	19,264,097

Recall that, SIFS detects the inactive features and samples in a static manner, i.e., we perform SIFS only once before the optimization and thus the size of the problem we need to perform optimization on is fixed. However, the method in [18] detects inactive features and samples in a dynamic manner [2], i.e., they perform their method along with the optimization and thus the size of the problem would keep decreasing during the iterative process. Thus, comparing SIFS with the method in [18] in terms of rejection ratios is inapplicable. We compare the performance of SIFS with the method in [18] in terms of speedup. Specifically, we compare the speedup gained by SIFS and the method in [18] for solving problem (P*) at 1000 pairs of parameter values. The code of the method in [18] is obtained from (<https://github.com/husk214/s3fs>).

Table 3: Running time (in seconds) for solving problem (P*) at 1000 pairs of parameter values on five real datasets.

Data Set	Solver	Method in [18]+Solver			SIFS+Solver		
		Screen	Solver	Speedup	Screen	Solver	Speedup
real-sim	3.93E+04	24.10	4.94E+03	7.91	60.01	140.25	195.00
rcv1-train	2.98E+04	10.00	3.73E+03	7.90	27.11	80.11	277.10
rcv1-test	1.10E+06	398.00	1.35E+05	8.10	1.17E+03	2.55E+03	295.11
url	—	3.18E+04	8.60E+05	—	7.66E+03	2.91E+04	—
kddb	—	4.31E+04	1.16E+06	—	1.10E+04	3.6E+04	—

Fig. 3 shows the rejection ratios of SIFS on the real-sim dataset (other results are in the supplementary material). In Fig. 3, we can see that some inactive features and samples are identified in the 2nd and 3rd triggering of ISS and IFS, which verifies the necessity of the alternating application of ISS and IFS. SIFS is efficient since it always stops in 3 times of

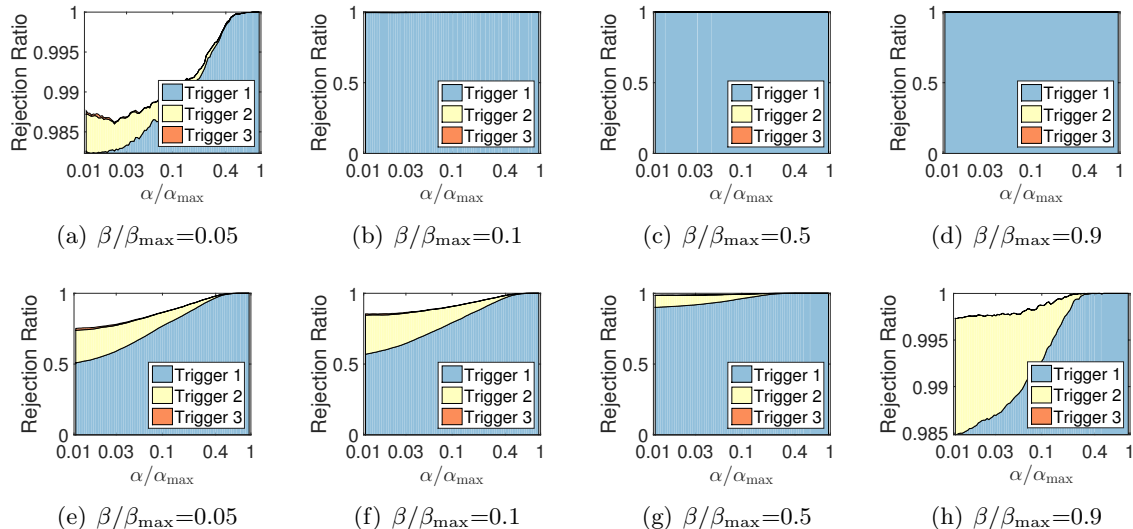


Figure 3: Rejection ratios of SIFS on the real-sim dataset (first row: Feature Screening, second row: Sample Screening).

triggering. In addition, most of ($> 98\%$) the inactive features can be identified in the 1st triggering of IFS while identifying inactive samples needs to apply ISS two or more times. It may result from two reasons: 1) We run ISS first, which reinforces the capability of IFS due to the synergy effect (see Sections 4.1 and 4.2), see Section A.12.1 in the supplementary material for further verification; 2) Feature screening here may be easier than sample screening.

Table 3 reports the running time of solver without and with the method in [18] and SIFS for solving problem (P*) at 1000 pairs of parameter values on real datasets. The speedup gained by SIFS is up to 300 times on real-sim, rcv1-train and rcv1-test. Moreover, SIFS significantly outperforms the method in [18] in terms of speedup—by about 30 to 40 times faster on the aforementioned three datasets. For datasets url and kddb, we do not report the results of the solver as the sizes of the datasets are huge and the computational cost is prohibitive. Instead, we can see that the solver with SIFS is about 25 times faster than the solver with the method in [18] on both datasets url and kddb. Take the dataset kddb as an example. The solver with SIFS takes about 13 hours to solve problem (P*) for all 1000 pairs of parameter values, while the solver with the method in [18] needs 11 days to finish the same task.

6 Conclusion

In this paper, we develop a novel data reduction method SIFS to simultaneously identify inactive features and samples for sparse SVM. Our major contribution is a novel framework for an accurate estimation of the primal and dual optima based on strong convexity. To the best of our knowledge, the proposed SIFS is the first static screening method that is able to simultaneously identify inactive features and samples for sparse SVMs. An appealing feature of SIFS is that all detected features and samples are guaranteed to be irrelevant to the outputs. Thus, the model learned on the reduced data is identical to the one learned on the full data. Experiments on both synthetic and real datasets demonstrate that SIFS can dramatically reduce the problem size and the resulting speedup can be orders of magnitude. We plan to generalize SIFS to more complicated models, e.g., SVM with a structured sparsity-inducing

penalty.

Acknowledgements

This work was supported by the National Basic Research Program of China (973 Program) under Grant 2013CB336500, National Natural Science Foundation of China under Grant 61233011 and National Youth Top-notch Talent Support Program.

References

- [1] Jinbo Bi, Kristin Bennett, Mark Embrechts, Curt Breneman, and Minghu Song. Dimensionality reduction via sparse support vector machines. *The Journal of Machine Learning Research*, 3:1229–1243, 2003.
- [2] Antoine Bonnefoy, Valentin Emiya, Liva Ralaivola, and Rémi Gribonval. A dynamic screening principle for the lasso. In *Signal Processing Conference (EUSIPCO), 2014 Proceedings of the 22nd European*, pages 6–10. IEEE, 2014.
- [3] Bryan Catanzaro, Narayanan Sundaram, and Kurt Keutzer. Fast support vector machine training and classification on graphics processors. In *Proceedings of the 25th international conference on Machine learning*, pages 104–111. ACM, 2008.
- [4] Chih-Chung Chang and Chih-Jen Lin. Libsvm: a library for support vector machines. *ACM Transactions on Intelligent Systems and Technology (TIST)*, 2(3):27, 2011.
- [5] Laurent El Ghaoui, Vivian Viallon, and Tarek Rabbani. Safe feature elimination in sparse supervised learning. *Pacific Journal of Optimization*, 8:667–698, 2012.
- [6] Rong-En Fan, Kai-Wei Chang, Cho-Jui Hsieh, Xiang-Rui Wang, and Chih-Jen Lin. Liblinear: A library for large linear classification. *The Journal of Machine Learning Research*, 9:1871–1874, 2008.
- [7] Trevor Hastie, Saharon Rosset, Robert Tibshirani, and Ji Zhu. The entire regularization path for the support vector machine. *The Journal of Machine Learning Research*, 5:1391–1415, 2004.
- [8] Trevor Hastie, Robert Tibshirani, and Martin Wainwright. *Statistical learning with sparsity: the lasso and generalizations*. CRC Press, 2015.
- [9] Cho-Jui Hsieh, Kai-Wei Chang, Chih-Jen Lin, S Sathiya Keerthi, and Sellamanickam Sundararajan. A dual coordinate descent method for large-scale linear svm. In *Proceedings of the 25th international conference on Machine learning*, pages 408–415. ACM, 2008.
- [10] Thorsten Joachims. *Text categorization with support vector machines: Learning with many relevant features*. Springer, 1998.
- [11] Irene Kotsia and Ioannis Pitas. Facial expression recognition in image sequences using geometric deformation features and support vector machines. *Image Processing, IEEE Transactions on*, 16(1):172–187, 2007.
- [12] Johannes Mohr and Klaus Obermayer. A topographic support vector machine: Classification using local label configurations. In *Advances in Neural Information Processing Systems*, pages 929–936, 2004.

- [13] Harikrishna Narasimhan and Shivani Agarwal. Svm pauc tight: a new support vector method for optimizing partial auc based on a tight convex upper bound. In *Proceedings of the 19th ACM SIGKDD international conference on Knowledge discovery and data mining*, pages 167–175. ACM, 2013.
- [14] Eugene Ndiaye, Olivier Fercoq, Alexandre Gramfort, and Joseph Salmon. Gap safe screening rules for sparse-group lasso. In D. D. Lee, M. Sugiyama, U. V. Luxburg, I. Guyon, and R. Garnett, editors, *Advances in Neural Information Processing Systems 29*, pages 388–396. Curran Associates, Inc., 2016.
- [15] Kohei Ogawa, Yoshiki Suzuki, and Ichiro Takeuchi. Safe screening of non-support vectors in pathwise svm computation. In *Proceedings of the 30th International Conference on Machine Learning*, pages 1382–1390, 2013.
- [16] Shai Shalev-Shwartz, Yoram Singer, Nathan Srebro, and Andrew Cotter. Pegasos: Primal estimated sub-gradient solver for svm. *Mathematical programming*, 127(1):3–30, 2011.
- [17] Shai Shalev-Shwartz and Tong Zhang. Accelerated proximal stochastic dual coordinate ascent for regularized loss minimization. *Mathematical Programming*, 155(1-2):105–145, 2016.
- [18] Atsushi Shibagaki, Masayuki Karasuyama, Kohei Hatano, and Ichiro Takeuchi. Simultaneous safe screening of features and samples in doubly sparse modeling. In *Proceedings of The 33rd International Conference on Machine Learning*, 2016.
- [19] Robert Tibshirani, Jacob Bien, Jerome Friedman, Trevor Hastie, Noah Simon, Jonathan Taylor, and Ryan J Tibshirani. Strong rules for discarding predictors in lasso-type problems. *Journal of the Royal Statistical Society: Series B (Statistical Methodology)*, 74(2):245–266, 2012.
- [20] Jie Wang, Jiayu Zhou, Jun Liu, Peter Wonka, and Jieping Ye. A safe screening rule for sparse logistic regression. In *Advances in Neural Information Processing Systems*, pages 1053–1061, 2014.
- [21] Jie Wang, Jiayu Zhou, Peter Wonka, and Jieping Ye. Lasso screening rules via dual polytope projection. In *Advances in Neural Information Processing Systems*, pages 1070–1078, 2013.
- [22] Li Wang, Ji Zhu, and Hui Zou. The doubly regularized support vector machine. *Statistica Sinica*, pages 589–615, 2006.
- [23] Zhen James Xiang and Peter J Ramadge. Fast lasso screening tests based on correlations. In *Acoustics, Speech and Signal Processing (ICASSP), 2012 IEEE International Conference on*, pages 2137–2140. IEEE, 2012.
- [24] Yuya Yoshikawa, Tomoharu Iwata, and Hiroshi Sawada. Latent support measure machines for bag-of-words data classification. In *Advances in Neural Information Processing Systems*, pages 1961–1969, 2014.

A Appendix

In this appendix, we first present the detailed proofs of all the theorems in the main text and then report the rest experiment results which are omitted in the experiment section due to the space limitation.

A.1 Proof for Theorem 1

Proof. of Theorem 1:

(i) : Let $\bar{\mathbf{X}} = (\bar{\mathbf{x}}_1, \bar{\mathbf{x}}_2, \dots, \bar{\mathbf{x}}_n)$ and $\mathbf{z} = \mathbf{1} - \bar{\mathbf{X}}^T \mathbf{w}$, the primal problem (P*) then is equivalent to

$$\begin{aligned} \min_{\mathbf{w} \in \mathbb{R}^p, \mathbf{z} \in \mathbb{R}^n} \quad & \frac{\alpha}{2} \|\mathbf{w}\|^2 + \beta \|\mathbf{w}\|_1 + \frac{1}{n} \sum_{i=1}^n \ell([\mathbf{z}]_i), \\ \text{s.t.} \quad & \mathbf{z} = \mathbf{1} - \bar{\mathbf{X}}^T \mathbf{w}. \end{aligned}$$

The Lagrangian then becomes

$$L(\mathbf{w}, \mathbf{z}, \theta) = \frac{\alpha}{2} \|\mathbf{w}\|^2 + \beta \|\mathbf{w}\|_1 + \frac{1}{n} \sum_{i=1}^n \ell([\mathbf{z}]_i) + \frac{1}{n} \langle \mathbf{1} - \bar{\mathbf{X}}^T \mathbf{w} - \mathbf{z}, \theta \rangle \quad (17)$$

$$\begin{aligned} &= \underbrace{\frac{\alpha}{2} \|\mathbf{w}\|^2 + \beta \|\mathbf{w}\|_1 - \frac{1}{n} \langle \bar{\mathbf{X}} \theta, \mathbf{w} \rangle}_{:=f_1(\mathbf{w})} + \underbrace{\frac{1}{n} \sum_{i=1}^n \ell([\mathbf{z}]_i) - \frac{1}{n} \langle \mathbf{z}, \theta \rangle + \frac{1}{n} \langle \mathbf{1}, \theta \rangle}_{:=f_2(\mathbf{z})} \end{aligned} \quad (18)$$

We first consider the subproblem $\min_{\mathbf{w}} L(\mathbf{w}, \mathbf{z}, \theta)$:

$$\begin{aligned} 0 \in \partial_{\mathbf{w}} L(\mathbf{w}, \mathbf{z}, \theta) &= \partial_{\mathbf{w}} f_1(\mathbf{w}) = \alpha \mathbf{w} - \frac{1}{n} \bar{\mathbf{X}} \theta + \beta \partial \|\mathbf{w}\|_1 \Leftrightarrow \\ \frac{1}{n} \bar{\mathbf{X}} \theta &\in \alpha \mathbf{w} + \beta \partial \|\mathbf{w}\|_1 \Rightarrow \mathbf{w} = \frac{1}{\alpha} \mathcal{S}_{\beta} \left(\frac{1}{n} \bar{\mathbf{X}} \theta \right) \end{aligned} \quad (19)$$

By substituting (19) into $f_1(\mathbf{w})$, we get

$$f_1(\mathbf{w}) = \frac{\alpha}{2} \|\mathbf{w}\|^2 + \beta \|\mathbf{w}\|_1 - \langle \alpha \mathbf{w} + \beta \partial \|\mathbf{w}\|_1, \mathbf{w} \rangle = -\frac{\alpha}{2} \|\mathbf{w}\|^2 = -\frac{1}{2\alpha} \|\mathcal{S}_{\beta} \left(\frac{1}{n} \bar{\mathbf{X}} \theta \right)\|^2. \quad (20)$$

Then, we consider the problem $\min_{\mathbf{z}} L(\mathbf{w}, \mathbf{z}, \theta)$:

$$\begin{aligned} 0 = \nabla_{[\mathbf{z}]_i} L(\mathbf{w}, \mathbf{z}, \theta) &= \nabla_{[\mathbf{z}]_i} f_2(\mathbf{z}) = \begin{cases} -\frac{1}{n} [\theta]_i, & \text{if } [\mathbf{z}]_i < 0, \\ \frac{1}{\gamma n} [\mathbf{z}]_i - \frac{1}{n} [\theta]_i, & \text{if } 0 \leq [\mathbf{z}]_i \leq \gamma, \\ \frac{1}{n} - \frac{1}{n} [\theta]_i, & \text{if } [\mathbf{z}]_i > \gamma. \end{cases} \\ \Rightarrow [\theta]_i &= \begin{cases} 0, & \text{if } [\mathbf{z}]_i < 0, \\ \frac{1}{\gamma} [\mathbf{z}]_i, & \text{if } 0 \leq [\mathbf{z}]_i \leq \gamma, \\ 1, & \text{if } [\mathbf{z}]_i > \gamma. \end{cases} \end{aligned} \quad (21)$$

Thus, we have

$$f_2(\mathbf{z}) = \begin{cases} -\frac{\gamma}{2n} \|\theta\|^2, & \text{if } [\theta]_i \in [0, 1], \forall i \in [n], \\ -\infty, & \text{otherwise.} \end{cases} \quad (22)$$

Combining Eqn (17), (20) and (22), we obtain the dual problem:

$$\min_{\theta \in [0,1]^n} \frac{1}{2\alpha} \|\mathcal{S}_{\beta} \left(\frac{1}{n} \bar{\mathbf{X}} \theta \right)\|^2 + \frac{\gamma}{2n} \|\theta\|^2 - \frac{1}{n} \langle \mathbf{1}, \theta \rangle \quad (23)$$

(ii) : From Eqn (19) and (21), we get the KKT conditions:

$$\begin{aligned} \mathbf{w}^*(\alpha, \beta) &= \frac{1}{\alpha} \mathcal{S}_\beta \left(\frac{1}{n} \bar{\mathbf{X}}^T \theta^*(\alpha, \beta) \right) \\ [\theta^*(\alpha, \beta)]_i &= \begin{cases} 0, & \text{if } 1 - \langle \bar{\mathbf{x}}_i, \mathbf{w}^*(\alpha, \beta) \rangle < 0, \\ \frac{1}{\gamma} (1 - \langle \bar{\mathbf{x}}_i, \mathbf{w}^*(\alpha, \beta) \rangle), & \text{if } 0 \leq 1 - \langle \bar{\mathbf{x}}_i, \mathbf{w}^*(\alpha, \beta) \rangle \leq \gamma, \\ 1, & \text{if } 1 - \langle \bar{\mathbf{x}}_i, \mathbf{w}^*(\alpha, \beta) \rangle > \gamma. \end{cases} \quad i = 1, \dots, n. \end{aligned}$$

The proof is complete. \square

A.2 Proof for Lemma 1

Proof. of Theorem 1:

- 1) It is the conclusion of the analysis above.
- 2) After feature screening, the primal problem (P*) is scaled into:

$$\min_{\tilde{\mathbf{w}} \in \mathbb{R}^{|\hat{\mathcal{F}}^c|}} \frac{\alpha}{2} \|\tilde{\mathbf{w}}\|^2 + \beta \|\tilde{\mathbf{w}}\|_1 + \frac{1}{n} \sum_{i=1}^n \ell(1 - \langle [\bar{\mathbf{x}}_i]_{\hat{\mathcal{F}}^c}, \tilde{\mathbf{w}} \rangle), \quad (\text{scaled-}P^*-1)$$

Thus, we can easily derive out the dual problem of (scaled- P^*-1):

$$\min_{\tilde{\theta} \in [0, \alpha]^n} \tilde{D}(\tilde{\theta}; \alpha, \beta) = \frac{1}{2\alpha} \|\mathcal{S}_\beta \left(\frac{1}{n} [\bar{\mathbf{X}}]_{\hat{\mathcal{F}}^c} \tilde{\theta} \right)\|^2 + \frac{\gamma}{2n} \|\tilde{\theta}\|^2 - \frac{1}{n} \langle \mathbf{1}, \tilde{\theta} \rangle. \quad (\text{scaled-}D^*-1)$$

and also the KKT conditions:

$$\begin{aligned} \tilde{\mathbf{w}}^*(\alpha, \beta) &= \frac{1}{\alpha} \mathcal{S}_\beta \left(\frac{1}{n} [\bar{\mathbf{X}}]_{\hat{\mathcal{F}}^c} \tilde{\theta}^*(\alpha, \beta) \right) \quad (\text{scaled-KKT-1}) \\ [\tilde{\theta}^*(\alpha, \beta)]_i &= \begin{cases} 0, & \text{if } 1 - \langle [\bar{\mathbf{x}}_i]_{\hat{\mathcal{F}}^c}, \tilde{\mathbf{w}}^*(\alpha, \beta) \rangle < 0, \\ \frac{1}{\gamma} (1 - \langle [\bar{\mathbf{x}}_i]_{\hat{\mathcal{F}}^c}, \tilde{\mathbf{w}}^*(\alpha, \beta) \rangle), & \text{if } 0 \leq 1 - \langle [\bar{\mathbf{x}}_i]_{\hat{\mathcal{F}}^c}, \tilde{\mathbf{w}}^*(\alpha, \beta) \rangle \leq \gamma, \\ 1, & \text{if } 1 - \langle [\bar{\mathbf{x}}_i]_{\hat{\mathcal{F}}^c}, \tilde{\mathbf{w}}^*(\alpha, \beta) \rangle > \gamma, \end{cases} \quad (\text{scaled-KKT-2}) \end{aligned}$$

Then, it is obvious that $\tilde{\mathbf{w}}^*(\alpha, \beta) = [\mathbf{w}^*(\alpha, \beta)]_{\hat{\mathcal{F}}^c}$, since essentially, problem (scaled- P^*-1) can be derived by substituting 0 to the weights for the eliminated features in (P*) and optimize over the rest weights.

Since the solutions $\mathbf{w}^*(\alpha, \beta)$ and $\theta^*(\alpha, \beta)$ satisfy the conditions (KKT-1) and (KKT-2) and $\langle [\bar{\mathbf{x}}_i]_{\hat{\mathcal{F}}^c}, \tilde{\mathbf{w}}^*(\alpha, \beta) \rangle = \langle \bar{\mathbf{x}}_i, \mathbf{w}^*(\alpha, \beta) \rangle$ for all i , we know $\tilde{\mathbf{w}}^*(\alpha, \beta)$ and $\tilde{\theta}^*(\alpha, \beta)$ satisfy the conditions (scaled-KKT-1) and (scaled-KKT-2). So they are the solutions of problems (scaled- P^*-1) and (scaled- D^*-1). Thus, due to the uniqueness of the solution of problem (scaled- D^*-1), we have

$$\theta^*(\alpha, \beta) = \tilde{\theta}^*(\alpha, \beta) \quad (24)$$

From 1) we have, $[\tilde{\theta}^*(\alpha, \beta)]_{\hat{\mathcal{R}}^c} = 0$ and $[\tilde{\theta}^*(\alpha, \beta)]_{\hat{\mathcal{L}}^c} = 1$. Therefore, from the dual problem (scaled- D^*), we can see that $[\hat{\theta}^*(C, \alpha)]_{\hat{\mathcal{D}}^c}$ can be recovered from the following problem:

$$\min_{\hat{\theta} \in [0, 1]^{|\hat{\mathcal{D}}^c|}} \frac{1}{2\alpha} \|\mathcal{S}_\beta \left(\frac{1}{n} \hat{\mathbf{G}}_1 \hat{\theta} + \frac{1}{n} \hat{\mathbf{G}}_2 \mathbf{1} \right)\|^2 + \frac{\gamma}{2n} \|\hat{\theta}\|^2 - \frac{1}{n} \langle \mathbf{1}, \hat{\theta} \rangle,$$

Since $[\tilde{\theta}^*(\alpha, \beta)]_{\hat{\mathcal{D}}^c} = [\theta^*(\alpha, \beta)]_{\hat{\mathcal{D}}^c}$, the proof is therefore completed. \square

A.3 Proof for Lemma 2

Proof. Due to the α -strong convexity of the objective $P(\mathbf{w}; \alpha, \beta)$, we have

$$P(\mathbf{w}^*(\alpha_0, \beta_0); \alpha, \beta) \geq P(\mathbf{w}^*(\alpha, \beta_0); \alpha, \beta) + \frac{\alpha}{2} \|\mathbf{w}^*(\alpha_0, \beta_0) - \mathbf{w}^*(\alpha, \beta_0)\|^2$$

$$P(\mathbf{w}^*(\alpha, \beta_0); \alpha_0, \beta) \geq P(\mathbf{w}^*(\alpha_0, \beta_0); \alpha_0, \beta) + \frac{\alpha_0}{2} \|\mathbf{w}^*(\alpha_0, \beta_0) - \mathbf{w}^*(\alpha, \beta_0)\|^2$$

which are equivalent to

$$\begin{aligned} & \frac{\alpha}{2} \|\mathbf{w}^*(\alpha_0, \beta_0)\|^2 + \beta_0 \|\mathbf{w}^*(\alpha_0, \beta_0)\|_1 + \frac{1}{n} \sum_{i=1}^n \ell(1 - \langle \bar{\mathbf{x}}_i, \mathbf{w}^*(\alpha_0, \beta_0) \rangle) \\ & \geq \frac{\alpha}{2} \|\mathbf{w}^*(\alpha, \beta_0)\|^2 + \beta_0 \|\mathbf{w}^*(\alpha, \beta_0)\|_1 + \frac{1}{n} \sum_{i=1}^n \ell(1 - \langle \bar{\mathbf{x}}_i, \mathbf{w}^*(\alpha, \beta_0) \rangle) \\ & \quad + \frac{\alpha}{2} \|\mathbf{w}^*(\alpha_0, \beta_0) - \mathbf{w}^*(\alpha, \beta_0)\|^2 \\ & \frac{\alpha_0}{2} \|\mathbf{w}^*(\alpha, \beta_0)\|^2 + \beta_0 \|\mathbf{w}^*(\alpha, \beta_0)\|_1 + \frac{1}{n} \sum_{i=1}^n \ell(1 - \langle \bar{\mathbf{x}}_i, \mathbf{w}^*(\alpha, \beta_0) \rangle) \\ & \geq \frac{\alpha_0}{2} \|\mathbf{w}^*(\alpha_0, \beta_0)\|^2 + \beta_0 \|\mathbf{w}^*(\alpha_0, \beta_0)\|_1 + \frac{1}{n} \sum_{i=1}^n \ell(1 - \langle \bar{\mathbf{x}}_i, \mathbf{w}^*(\alpha_0, \beta_0) \rangle) \\ & \quad + \frac{\alpha_0}{2} \|\mathbf{w}^*(\alpha_0, \beta_0) - \mathbf{w}^*(\alpha, \beta_0)\|^2 \end{aligned}$$

Adding the above two inequalities together, we get

$$\begin{aligned} & \frac{\alpha - \alpha_0}{2} \|\mathbf{w}^*(\alpha_0, \beta_0)\|^2 \geq \frac{\alpha - \alpha_0}{2} \|\mathbf{w}^*(\alpha, \beta_0)\|^2 + \frac{\alpha_0 + \alpha}{2} \|\mathbf{w}^*(\alpha_0, \beta_0) - \mathbf{w}^*(\alpha, \beta_0)\|^2 \\ \Rightarrow & \|\mathbf{w}^*(\alpha, \beta_0) - \frac{\alpha_0 + \alpha}{2\alpha} \mathbf{w}^*(\alpha_0, \beta_0)\|^2 \leq \frac{(\alpha - \alpha_0)^2}{4\alpha^2} \|\mathbf{w}^*(\alpha_0, \beta_0)\|^2 \end{aligned} \quad (25)$$

Substitute the prior that $[\mathbf{w}^*(\alpha, \beta_0)]_{\hat{\mathcal{F}}} = 0$ into (25), we get

$$\begin{aligned} & \|[\mathbf{w}^*(\alpha, \beta_0)]_{\hat{\mathcal{F}}^c} - \frac{\alpha_0 + \alpha}{2\alpha} [\mathbf{w}^*(\alpha_0, \beta_0)]_{\hat{\mathcal{F}}^c}\|^2 \\ & \leq \frac{(\alpha - \alpha_0)^2}{4\alpha^2} \|\mathbf{w}^*(\alpha_0, \beta_0)\|^2 - \frac{(\alpha_0 + \alpha)^2}{4\alpha^2} \|[\mathbf{w}^*(\alpha_0, \beta_0)]_{\hat{\mathcal{F}}}\|^2. \end{aligned}$$

The proof is complete. \square

A.4 Proof for Lemma 3

Proof. Firstly, we need to extend the definition of $D(\theta; \alpha, \beta)$ to \mathbb{R}^n :

$$\tilde{D}(\theta; \alpha, \beta) = \begin{cases} D(\theta; \alpha, \beta), & \text{if } \theta \in [0, 1]^n, \\ +\infty, & \text{otherwise} \end{cases} \quad (26)$$

Due to the strong convexity of objective $\tilde{D}(\theta; \alpha, \beta)$, we have

$$\begin{aligned} \tilde{D}(\theta^*(\alpha_0, \beta_0), \alpha, \beta) & \geq \tilde{D}(\theta^*(\alpha, \beta_0), \alpha, \beta) + \frac{\gamma}{2n} \|\theta^*(\alpha_0, \beta_0) - \theta^*(\alpha, \beta_0)\|^2, \\ \tilde{D}(\theta^*(\alpha, \beta_0), \alpha_0, \beta) & \geq \tilde{D}(\theta^*(\alpha_0, \beta_0), \alpha_0, \beta) + \frac{\gamma}{2n} \|\theta^*(\alpha_0, \beta_0) - \theta^*(\alpha, \beta_0)\|^2. \end{aligned}$$

Since $\theta^*(\alpha_0, \beta_0), \theta^*(\alpha, \beta_0) \in [0, 1]^n$, the above inequalities are equivalent to

$$\begin{aligned} & \frac{1}{2\alpha} \|\mathcal{S}_{\beta_0}(\frac{1}{n} \bar{\mathbf{X}}^T \theta^*(\alpha_0, \beta_0))\|^2 + \frac{\gamma}{2n} \|\theta^*(\alpha_0, \beta_0)\|^2 - \frac{1}{n} \langle \mathbf{1}, \theta^*(\alpha_0, \beta_0) \rangle \\ & \geq \frac{1}{2\alpha} \|\mathcal{S}_{\beta_0}(\frac{1}{n} \bar{\mathbf{X}}^T \theta^*(\alpha, \beta_0))\|^2 + \frac{\gamma}{2n} \|\theta^*(\alpha, \beta_0)\|^2 - \frac{1}{n} \langle \mathbf{1}, \theta^*(\alpha, \beta_0) \rangle \\ & \quad + \frac{\gamma}{2n} \|\theta^*(\alpha_0, \beta_0) - \theta^*(\alpha, \beta_0)\|^2, \end{aligned}$$

$$\begin{aligned} & \frac{1}{2\alpha_0} \|\mathcal{S}_{\beta_0}(\frac{1}{n} \bar{\mathbf{X}}^T \theta^*(\alpha, \beta_0))\|^2 + \frac{\gamma}{2n} \|\theta^*(\alpha, \beta_0)\|^2 - \frac{1}{n} \langle \mathbf{1}, \theta^*(\alpha, \beta_0) \rangle \\ & \geq \frac{1}{2\alpha_0} \|\mathcal{S}_{\beta_0}(\frac{1}{n} \bar{\mathbf{X}}^T \theta^*(\alpha_0, \beta_0))\|^2 + \frac{\gamma}{2n} \|\theta^*(\alpha_0, \beta_0)\|^2 - \frac{1}{n} \langle \mathbf{1}, \theta^*(\alpha_0, \beta_0) \rangle + \frac{\gamma}{2n} \|\theta^*(\alpha_0, \beta_0) - \theta^*(\alpha, \beta_0)\|^2. \end{aligned}$$

Adding the above two inequalities, we get

$$\begin{aligned} & \frac{\gamma(\alpha - \alpha_0)}{2n} \|\theta^*(\alpha_0, \beta_0)\|^2 - \frac{\alpha - \alpha_0}{n} \langle \mathbf{1}, \theta^*(\alpha_0, \beta_0) \rangle \\ & \geq \frac{\gamma(\alpha - \alpha_0)}{2n} \|\theta^*(\alpha, \beta_0)\|^2 - \frac{\alpha - \alpha_0}{n} \langle \mathbf{1}, \theta^*(\alpha, \beta_0) \rangle + \frac{\gamma(\alpha_0 + \alpha)}{2n} \|\theta^*(\alpha_0, \beta_0) - \theta^*(\alpha, \beta_0)\|^2 \end{aligned}$$

That is equivalent to

$$\begin{aligned} & \|\theta^*(\alpha, \beta_0)\|^2 - \langle \frac{\alpha - \alpha_0}{\gamma\alpha} \mathbf{1} + \frac{\alpha_0 + \alpha}{\alpha} \theta^*(\alpha_0, \beta_0), \theta^*(\alpha, \beta_0) \rangle \\ & \leq -\frac{\alpha_0}{\alpha} \|\theta^*(\alpha_0, \beta_0)\|^2 - \frac{\alpha - \alpha_0}{\gamma\alpha} \langle \mathbf{1}, \theta^*(\alpha_0, \beta_0) \rangle \end{aligned} \quad (27)$$

That is

$$\|\theta^*(\alpha, \beta_0) - (\frac{\alpha - \alpha_0}{2\gamma\alpha} \mathbf{1} + \frac{\alpha_0 + \alpha}{2\alpha} \theta^*(\alpha_0, \beta_0))\|^2 \leq (\frac{\alpha - \alpha_0}{2\alpha})^2 \|\theta^*(\alpha_0, \beta_0) - \frac{1}{\gamma} \mathbf{1}\|^2 \quad (28)$$

Substitute the priors that $[\theta^*(\alpha, \beta_0)]_{\hat{\mathcal{R}}} = 0$ and $[\theta^*(\alpha, \beta_0)]_{\hat{\mathcal{L}}} = 1$ into (28), we have

$$\begin{aligned} & \|[\theta^*(\alpha, \beta_0)]_{\hat{\mathcal{D}}^c} - (\frac{\alpha - \alpha_0}{2\gamma\alpha} \mathbf{1} + \frac{\alpha_0 + \alpha}{2\alpha} [\theta^*(\alpha_0, \beta_0)]_{\hat{\mathcal{D}}^c})\|^2 \\ & \leq (\frac{\alpha - \alpha_0}{2\alpha})^2 \|\theta^*(\alpha_0, \beta_0) - \frac{1}{\gamma} \mathbf{1}\|^2 - \|\frac{(2\gamma - 1)\alpha + \alpha_0}{2\gamma\alpha} \mathbf{1} - \frac{\alpha_0 + \alpha}{2\alpha} [\theta^*(\alpha_0, \beta_0)]_{\hat{\mathcal{L}}}\|^2 \\ & \quad - \|\frac{\alpha - \alpha_0}{2\gamma\alpha} \mathbf{1} + \frac{\alpha_0 + \alpha}{2\alpha} [\theta^*(\alpha_0, \beta_0)]_{\hat{\mathcal{R}}}\|^2. \end{aligned}$$

The proof is complete. \square

A.5 Proof for Lemma 4

Before the proof of Lemma 4, we should prove that the optimization problem in (1) is equivalent to

$$s^i(\alpha, \beta_0) = \max_{\theta \in \Theta} \left\{ \frac{1}{n} |\langle [\bar{\mathbf{x}}^i]_{\hat{\mathcal{D}}^c}, \theta \rangle + \langle [\bar{\mathbf{x}}^i]_{\hat{\mathcal{L}}}, \mathbf{1} \rangle| \right\}, i \in \hat{\mathcal{F}}^c. \quad (29)$$

To avoid notational confusion, we denote the feasible region Θ in (1) as $\tilde{\Theta}$. Then,

$$\begin{aligned} & \max_{\theta \in \tilde{\Theta}} \left\{ \left| \frac{1}{n} [\bar{\mathbf{X}}\theta]_i \right| \right\} = \max_{\theta \in \tilde{\Theta}} \left\{ \frac{1}{n} |\bar{\mathbf{x}}^i \theta| \right\} \\ & = \max_{\theta \in \tilde{\Theta}} \left\{ \frac{1}{n} |[\bar{\mathbf{x}}^i]_{\hat{\mathcal{D}}^c} [\theta]_{\hat{\mathcal{D}}^c} + [\bar{\mathbf{x}}^i]_{\hat{\mathcal{L}}} [\theta]_{\hat{\mathcal{L}}} + [\bar{\mathbf{x}}^i]_{\hat{\mathcal{R}}} [\theta]_{\hat{\mathcal{R}}}| \right\} \\ & = \max_{\theta \in \tilde{\Theta}} \left\{ \frac{1}{n} |\langle [\bar{\mathbf{x}}^i]_{\hat{\mathcal{D}}^c}, [\theta]_{\hat{\mathcal{D}}^c} \rangle + \langle [\bar{\mathbf{x}}^i]_{\hat{\mathcal{L}}}, \mathbf{1} \rangle| \right\} = s^i(\alpha, \beta_0). \end{aligned}$$

The last equation holds since $[\theta]_{\hat{\mathcal{L}}} = \mathbf{1}$, $[\theta]_{\hat{\mathcal{R}}} = 0$ and $[\theta]_{\hat{\mathcal{D}}^c} \in \Theta$.

Proof. of Lemma 4:

$$\begin{aligned} s^i(\alpha, \beta_0) &= \max_{\theta \in B(\mathbf{c}, r)} \left\{ \frac{1}{n} |\langle [\bar{\mathbf{x}}^i]_{\hat{\mathcal{D}}^c}, \theta \rangle + \langle [\bar{\mathbf{x}}^i]_{\hat{\mathcal{L}}}, \mathbf{1} \rangle| \right\} \\ &= \max_{\eta \in B(\mathbf{0}, r)} \left\{ \frac{1}{n} |\langle [\bar{\mathbf{x}}^i]_{\hat{\mathcal{D}}^c}, \mathbf{c} \rangle + \langle [\bar{\mathbf{x}}^i]_{\hat{\mathcal{L}}}, \mathbf{1} \rangle + \langle [\bar{\mathbf{x}}^i]_{\hat{\mathcal{D}}^c}, \eta \rangle| \right\} \\ &= \frac{1}{n} (|\langle [\bar{\mathbf{x}}^i]_{\hat{\mathcal{D}}^c}, \mathbf{c} \rangle + \langle [\bar{\mathbf{x}}^i]_{\hat{\mathcal{L}}}, \mathbf{1} \rangle| + \|[\bar{\mathbf{x}}^i]_{\hat{\mathcal{D}}^c}\| r) \end{aligned}$$

The last equality holds since $-\|[\bar{\mathbf{x}}^i]_{\hat{\mathcal{D}}^c}\| r \leq \langle [\bar{\mathbf{x}}^i]_{\hat{\mathcal{D}}^c}, \eta \rangle \leq \|[\bar{\mathbf{x}}^i]_{\hat{\mathcal{D}}^c}\| r$. The proof is complete. \square

A.6 Proof for Theorem 4

Proof. (1) It can be obtained from the the rule (R1).

(2) It is from the definition of $\hat{\mathcal{F}}$. \square

A.7 Proof for Lemma 5

Firstly, we need to point out that the optimization problems in (2) and (3) are equivalent to the problems:

$$u_i(\alpha, \beta_0) = \max_{\mathbf{w} \in \mathcal{W}} \{1 - \langle [\bar{\mathbf{x}}_i]_{\hat{\mathcal{F}}^c}, \mathbf{w} \rangle\}, i \in \hat{\mathcal{D}}^c, \quad (30)$$

$$l_i(\alpha, \beta_0) = \min_{\mathbf{w} \in \mathcal{W}} \{1 - \langle [\bar{\mathbf{x}}_i]_{\hat{\mathcal{F}}^c}, \mathbf{w} \rangle\}, i \in \hat{\mathcal{D}}^c \quad (31)$$

They follow from the fact that $[\mathbf{w}]_{\hat{\mathcal{F}}^c} \in \mathcal{W}$ and

$$\begin{aligned} &\{1 - \langle \mathbf{w}, \bar{\mathbf{x}}_i \rangle\} \\ &= \{1 - \langle [\mathbf{w}]_{\hat{\mathcal{F}}^c}, [\bar{\mathbf{x}}_i]_{\hat{\mathcal{F}}^c} \rangle - \langle [\mathbf{w}]_{\hat{\mathcal{F}}}, [\bar{\mathbf{x}}_i]_{\hat{\mathcal{F}}} \rangle\} \\ &= \{1 - \langle [\mathbf{w}]_{\hat{\mathcal{F}}^c}, [\bar{\mathbf{x}}_i]_{\hat{\mathcal{F}}^c} \rangle\} \text{ (since } [\mathbf{w}]_{\hat{\mathcal{F}}} = 0\text{)}. \end{aligned}$$

Proof. of Lemma 5:

$$\begin{aligned} u_i(\alpha, \beta_0) &= \max_{\mathbf{w} \in B(\mathbf{c}, r)} \{1 - \langle [\bar{\mathbf{x}}_i]_{\hat{\mathcal{F}}^c}, \mathbf{w} \rangle\} \\ &= \max_{\eta \in B(\mathbf{0}, r)} \{1 - \langle [\bar{\mathbf{x}}_i]_{\hat{\mathcal{F}}^c}, \mathbf{c} \rangle - \langle [\bar{\mathbf{x}}_i]_{\hat{\mathcal{F}}^c}, \eta \rangle\} \\ &= 1 - \langle [\bar{\mathbf{x}}_i]_{\hat{\mathcal{F}}^c}, \mathbf{c} \rangle + \max_{\eta \in B(\mathbf{0}, r)} \{-\langle [\bar{\mathbf{x}}_i]_{\hat{\mathcal{F}}^c}, \eta \rangle\} \\ &= 1 - \langle [\bar{\mathbf{x}}_i]_{\hat{\mathcal{F}}^c}, \mathbf{c} \rangle + \|[\bar{\mathbf{x}}_i]_{\hat{\mathcal{F}}^c}\| r \end{aligned}$$

$$\begin{aligned} l_i(\alpha, \beta_0) &= \min_{\mathbf{w} \in B(\mathbf{c}, r)} \{1 - \langle [\bar{\mathbf{x}}_i]_{\hat{\mathcal{F}}^c}, \mathbf{w} \rangle\} \\ &= \min_{\eta \in B(\mathbf{0}, r)} \{1 - \langle [\bar{\mathbf{x}}_i]_{\hat{\mathcal{F}}^c}, \mathbf{c} \rangle - \langle [\bar{\mathbf{x}}_i]_{\hat{\mathcal{F}}^c}, \eta \rangle\} \\ &= 1 - \langle [\bar{\mathbf{x}}_i]_{\hat{\mathcal{F}}^c}, \mathbf{c} \rangle + \min_{\eta \in B(\mathbf{0}, r)} \{-\langle [\bar{\mathbf{x}}_i]_{\hat{\mathcal{F}}^c}, \eta \rangle\} \\ &= 1 - \langle [\bar{\mathbf{x}}_i]_{\hat{\mathcal{F}}^c}, \mathbf{c} \rangle - \|[\bar{\mathbf{x}}_i]_{\hat{\mathcal{F}}^c}\| r \end{aligned}$$

The proof is complete. \square

A.8 Proof for Theorem 5

Proof. (1) It can be obtained from the the rule (R2).
(2) It is from the definitions of $\hat{\mathcal{R}}$ and $\hat{\mathcal{L}}$.

□

A.9 Proof for Theorem 2

Proof. of Theorem 2:

We prove this theorem by verifying that the solutions $\mathbf{w}^*(\alpha, \beta) = \mathbf{0}$ and $\theta^*(\alpha, \beta) = \mathbf{1}$ satisfy the conditions (KKT-1) and (KKT-2).

Firstly, since $\beta \geq \beta_{\max} = \|\frac{1}{n}\bar{\mathbf{X}}\mathbf{1}\|_{\infty}$, we have $\mathcal{S}_{\beta}(\frac{1}{n}\bar{\mathbf{X}}\mathbf{1}) = 0$. Thus $\mathbf{w}^*(\alpha, \beta) = \mathbf{0}$ and $\theta^*(\alpha, \beta) = \mathbf{1}$ satisfy the condition (KKT-1).

Then, for all $i \in [n]$, we have

$$1 - \langle \bar{\mathbf{x}}_i, \mathbf{w}^*(\alpha, \beta) \rangle = 1 - 0 > \gamma.$$

Thus $\mathbf{w}^*(\alpha, \beta) = \mathbf{0}$ and $\theta^*(\alpha, \beta) = \mathbf{1}$ satisfy the condition (KKT-2). Hence, they are the solutions for the primal problem (P*) and the dual problem (D*), respectively. □

A.10 Proof for Theorem 3

Proof. of Theorem 3:

Similar with the proof of Theorem 2, we prove this theorem by verifying that the solutions $\mathbf{w}^*(\alpha, \beta) = \frac{1}{\alpha}\mathcal{S}_{\beta}(\frac{1}{n}\bar{\mathbf{X}}\theta^*(\alpha, \beta))$ and $\theta^*(\alpha, \beta) = \mathbf{1}$ satisfy the conditions (KKT-1) and (KKT-2).

1. **Case 1:** $\alpha_{\max}(\beta) \leq 0$. Then for all $\alpha > 0$, we have

$$\begin{aligned} & \min_{i \in [n]} \{1 - \langle \bar{\mathbf{x}}_i, \mathbf{w}^*(\alpha, \beta) \rangle\} \\ &= \min_{i \in [n]} \left\{1 - \frac{1}{\alpha} \langle \bar{\mathbf{x}}_i, \mathcal{S}_{\beta}(\frac{1}{n}\bar{\mathbf{X}}\theta^*(\alpha, \beta)) \rangle\right\} = \min_{i \in [n]} \left\{1 - \frac{1}{\alpha} \langle \bar{\mathbf{x}}_i, \mathcal{S}_{\beta}(\frac{1}{n}\bar{\mathbf{X}}\mathbf{1}) \rangle\right\} \\ &= 1 - \frac{1}{\alpha} \max_{i \in [n]} \langle \bar{\mathbf{x}}_i, \mathcal{S}_{\beta}(\frac{1}{n}\bar{\mathbf{X}}\mathbf{1}) \rangle = 1 - (1 - \gamma) \frac{1}{\alpha} \alpha_{\max}(\beta) \\ &\geq 1 > \gamma \end{aligned}$$

Then, $\mathcal{L} = [n]$ and $\mathbf{w}^*(\alpha, \beta) = \frac{1}{\alpha}\mathcal{S}_{\beta}(\frac{1}{n}\bar{\mathbf{X}}\theta^*(\alpha, \beta))$ and $\theta^*(\alpha, \beta) = \mathbf{1}$ satisfy the conditions (KKT-1) and (KKT-2). Hence, they are the optimal solution for the primal and dual problems (P*) and (D*).

2. **Case 2:** $\alpha_{\max}(\beta) > 0$. Then for any $\alpha \geq \alpha_{\max}(\beta)$, we have

$$\begin{aligned} & \min_{i \in [n]} \{1 - \langle \bar{\mathbf{x}}_i, \mathbf{w}^*(\alpha, \beta) \rangle\} \\ &= \min_{i \in [n]} \left\{1 - \frac{1}{\alpha} \langle \bar{\mathbf{x}}_i, \mathcal{S}_{\beta}(\frac{1}{n}\bar{\mathbf{X}}\theta^*(\alpha, \beta)) \rangle\right\} = \min_{i \in [n]} \left\{1 - \frac{1}{\alpha} \langle \bar{\mathbf{x}}_i, \mathcal{S}_{\beta}(\frac{1}{n}\bar{\mathbf{X}}\mathbf{1}) \rangle\right\} \\ &= 1 - \frac{1}{\alpha} \max_{i \in [n]} \langle \bar{\mathbf{x}}_i, \mathcal{S}_{\beta}(\frac{1}{n}\bar{\mathbf{X}}\mathbf{1}) \rangle = 1 - (1 - \gamma) \frac{1}{\alpha} \alpha_{\max}(\beta) \geq 1 - (1 - \gamma) = \gamma. \end{aligned}$$

Thus, $\mathcal{E} \cup \mathcal{L} = [n]$ and $\mathbf{w}^*(\alpha, \beta) = \frac{1}{\alpha}\mathcal{S}_{\beta}(\frac{1}{n}\bar{\mathbf{X}}\theta^*(\alpha, \beta))$ and $\theta^*(\alpha, \beta) = \mathbf{1}$ satisfy the conditions (KKT-1) and (KKT-2). Hence, they are the optimal solution for the primal and dual problems (P*) and (D*).

The proof is complete. □

A.11 Proof for Theorem 6

Proof. of Theorem 6:

(1) Given the reference solutions pair $\mathbf{w}^*(\alpha_{i-1,j}, \beta_j)$ and $\theta^*(\alpha_{i-1,j}, \beta_j)$, if we do ISS first in SIFS and apply ISS and IFS for infinite times. If after p times of triggering, no new inactive features or samples are identified, then we can denote the sequence of $\hat{\mathcal{F}}, \hat{\mathcal{R}}$ and $\hat{\mathcal{L}}$ as:

$$\hat{\mathcal{F}}_0^A = \hat{\mathcal{R}}_0^A = \hat{\mathcal{L}}_0^A = \emptyset \xrightarrow{ISS} \hat{\mathcal{F}}_1^A, \hat{\mathcal{R}}_1^A, \hat{\mathcal{L}}_1^A \xrightarrow{IFS} \hat{\mathcal{F}}_2^A, \hat{\mathcal{R}}_2^A, \hat{\mathcal{L}}_2^A \xrightarrow{ISS} \dots \hat{\mathcal{F}}_p^A, \hat{\mathcal{R}}_p^A, \hat{\mathcal{L}}_p^A \xrightarrow{IFS/ISS} \dots \quad (32)$$

$$\text{with } \hat{\mathcal{F}}_p^A = \hat{\mathcal{F}}_{p+1}^A = \hat{\mathcal{F}}_{p+2}^A = \dots, \hat{\mathcal{R}}_p^A = \hat{\mathcal{R}}_{p+1}^A = \hat{\mathcal{R}}_{p+2}^A = \dots, \text{ and } \hat{\mathcal{L}}_p^A = \hat{\mathcal{L}}_{p+1}^A = \hat{\mathcal{L}}_{p+2}^A = \dots \quad (33)$$

In the same way, if we do IFS first in SIFS and no new inactive feature or samples are identified after q times of triggering of ISS and IFS, then the sequence can be denoted as:

$$\hat{\mathcal{F}}_0^B = \hat{\mathcal{R}}_0^B = \hat{\mathcal{L}}_0^B = \emptyset \xrightarrow{IFS} \hat{\mathcal{F}}_1^B, \hat{\mathcal{R}}_1^B, \hat{\mathcal{L}}_1^B \xrightarrow{ISS} \hat{\mathcal{F}}_2^B, \hat{\mathcal{R}}_2^B, \hat{\mathcal{L}}_2^B \xrightarrow{IFS} \dots \hat{\mathcal{F}}_q^B, \hat{\mathcal{R}}_q^B, \hat{\mathcal{L}}_q^B \xrightarrow{IFS/ISS} \dots \quad (34)$$

$$\text{with } \hat{\mathcal{F}}_q^B = \hat{\mathcal{F}}_{q+1}^B = \hat{\mathcal{F}}_{q+2}^B = \dots, \hat{\mathcal{R}}_q^B = \hat{\mathcal{R}}_{q+1}^B = \hat{\mathcal{R}}_{q+2}^B = \dots, \text{ and } \hat{\mathcal{L}}_q^B = \hat{\mathcal{L}}_{q+1}^B = \hat{\mathcal{L}}_{q+2}^B = \dots \quad (35)$$

We first prove that $\hat{\mathcal{F}}_k^B \subseteq \hat{\mathcal{F}}_{k+1}^A, \hat{\mathcal{R}}_k^B \subseteq \hat{\mathcal{R}}_{k+1}^A$ and $\hat{\mathcal{L}}_k^B \subseteq \hat{\mathcal{L}}_{k+1}^A$ hold for all $k \geq 0$ by induction.

1) When $k = 0$, the equalities $\hat{\mathcal{F}}_0^B \subseteq \hat{\mathcal{F}}_1^A, \hat{\mathcal{R}}_0^B \subseteq \hat{\mathcal{R}}_1^A$ and $\hat{\mathcal{L}}_0^B \subseteq \hat{\mathcal{L}}_1^A$ hold since $\hat{\mathcal{F}}_0^B = \hat{\mathcal{R}}_0^B = \hat{\mathcal{L}}_0^B = \emptyset$.

2) If $\hat{\mathcal{F}}_k^B \subseteq \hat{\mathcal{F}}_{k+1}^A, \hat{\mathcal{R}}_k^B \subseteq \hat{\mathcal{R}}_{k+1}^A$ and $\hat{\mathcal{L}}_k^B \subseteq \hat{\mathcal{L}}_{k+1}^A$ hold, by the synergy effect of ISS and IFS, we have $\hat{\mathcal{F}}_{k+1}^B \subseteq \hat{\mathcal{F}}_{k+2}^A, \hat{\mathcal{R}}_{k+1}^B \subseteq \hat{\mathcal{R}}_{k+2}^A$ and $\hat{\mathcal{L}}_{k+1}^B \subseteq \hat{\mathcal{L}}_{k+2}^A$ hold.

Thus, $\hat{\mathcal{F}}_k^B \subseteq \hat{\mathcal{F}}_{k+1}^A, \hat{\mathcal{R}}_k^B \subseteq \hat{\mathcal{R}}_{k+1}^A$ and $\hat{\mathcal{L}}_k^B \subseteq \hat{\mathcal{L}}_{k+1}^A$ hold for all $k \geq 0$.

Similar with the analysis in (1), we can also prove that $\hat{\mathcal{F}}_k^A \subseteq \hat{\mathcal{F}}_{k+1}^B, \hat{\mathcal{R}}_k^A \subseteq \hat{\mathcal{R}}_{k+1}^B$ and $\hat{\mathcal{L}}_k^A \subseteq \hat{\mathcal{L}}_{k+1}^B$ hold for all $k \geq 0$.

Combine (1) and (2), we can get

$$\hat{\mathcal{F}}_0^B \subseteq \hat{\mathcal{F}}_1^A \subseteq \hat{\mathcal{F}}_2^B \subseteq \hat{\mathcal{F}}_3^A \dots \quad (36)$$

$$\hat{\mathcal{F}}_0^A \subseteq \hat{\mathcal{F}}_1^B \subseteq \hat{\mathcal{F}}_2^A \subseteq \hat{\mathcal{F}}_3^B \dots \quad (37)$$

$$\hat{\mathcal{R}}_0^B \subseteq \hat{\mathcal{R}}_1^A \subseteq \hat{\mathcal{R}}_2^B \subseteq \hat{\mathcal{R}}_3^A \dots \quad (38)$$

$$\hat{\mathcal{R}}_0^A \subseteq \hat{\mathcal{R}}_1^B \subseteq \hat{\mathcal{R}}_2^A \subseteq \hat{\mathcal{R}}_3^B \dots \quad (39)$$

$$\hat{\mathcal{L}}_0^B \subseteq \hat{\mathcal{L}}_1^A \subseteq \hat{\mathcal{L}}_2^B \subseteq \hat{\mathcal{L}}_3^A \dots \quad (40)$$

$$\hat{\mathcal{L}}_0^A \subseteq \hat{\mathcal{L}}_1^B \subseteq \hat{\mathcal{L}}_2^A \subseteq \hat{\mathcal{L}}_3^B \dots \quad (41)$$

by the first equality of (33), (36) and (37), we can get $\hat{\mathcal{F}}_p^A = \hat{\mathcal{F}}_q^B$. Similarly, we can get $\hat{\mathcal{R}}_p^A = \hat{\mathcal{R}}_q^B$ and $\hat{\mathcal{L}}_p^A = \hat{\mathcal{L}}_q^B$.

(2) If p is odd, then by (36), (38 and (40), we have $\hat{\mathcal{F}}_p^A \subseteq \hat{\mathcal{F}}_{p+1}^B, \hat{\mathcal{R}}_p^A \subseteq \hat{\mathcal{R}}_{p+1}^B$ and $\hat{\mathcal{L}}_p^A \subseteq \hat{\mathcal{L}}_{p+1}^B$. Thus $q \leq p + 1$.

Else if p is even, then by (37), (39) and (41), we have $\hat{\mathcal{F}}_p^A \subseteq \hat{\mathcal{F}}_{p+1}^B, \hat{\mathcal{R}}_p^A \subseteq \hat{\mathcal{R}}_{p+1}^B$ and $\hat{\mathcal{L}}_p^A \subseteq \hat{\mathcal{L}}_{p+1}^B$. Thus $q \leq p + 1$.

Do the same analysis for q , we can get $p \leq q + 1$.

Hence, $|p - q| \leq 1$.

The proof is complete. \square

A.12 Experiment Result

A.12.1 Verification of the Synergy Effect

Here, we verify the synergy effect between ISS and IFS in SIFS from the experiment results on the dataset real-sim. In Fig. 4, SIFS performs ISS (sample screening) first, while in Fig. 5, it performs IFS (feature screening) first. All the rejection ratios (Fig. 4(a)-(d)) of the 1st triggering of IFS when SIFS performs ISS first are much higher than (at least equal to) those (Fig. 5(a)-(d)) when SIFS performs IFS first. In turn, all the rejection ratios (Fig. 5(e)-(h)) of the 1st triggering of ISS when SIFS performs IFS first are also much higher than those (Fig. 4(e)-(h)) when SIFS performs ISS first. This demonstrates that the screening result of ISS can reinforce the capability of IFS and vice versa, which is the so called synergy effect. At last, in Fig. 5 and Fig. 4, we can see that the overall rejection ratios at the end of SIFS are the same, so no matter which (ISS or IFS) we perform first in SIFS, SIFS has the same screening performances in the end.

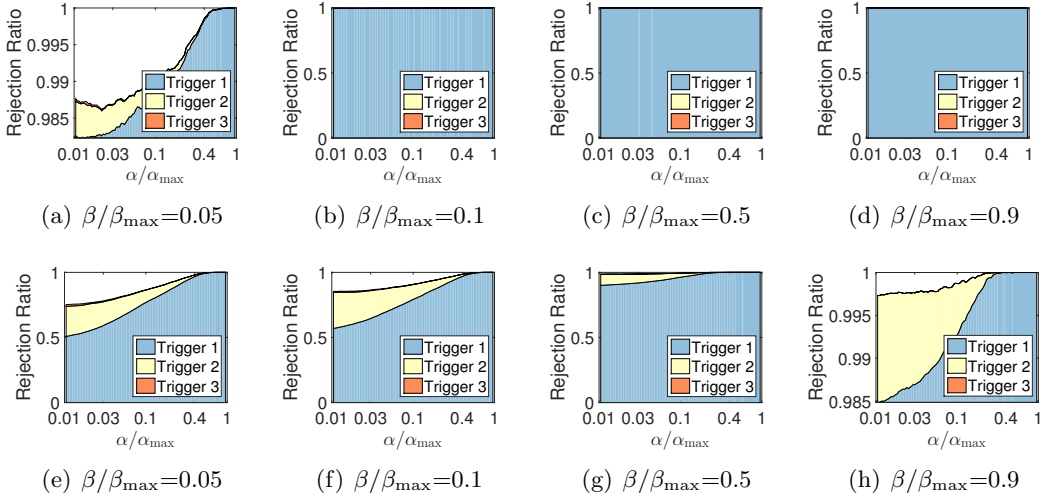


Figure 4: Rejection ratios of SIFS on real-sim when it performs **ISS** first (first row: Feature Screening, second row: Sample Screening).

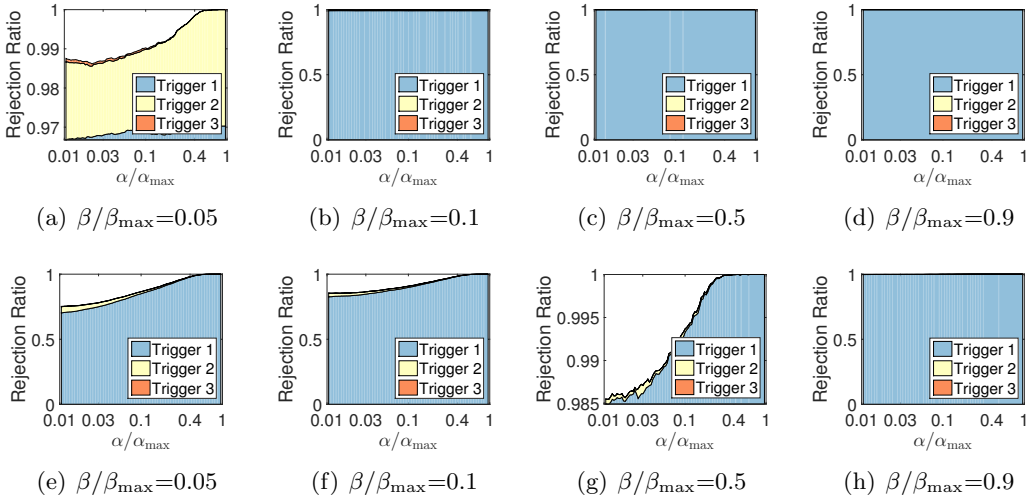


Figure 5: Rejection ratios of SIFS on real-sim when it performs **IFS** first (first row: Feature Screening, second row: Sample Screening).

A.12.2 The Rest Experiment Result

Below, we report the rejection ratios of SIFS on syn1 (Fig. 6), syn3 (Fig. 7), rcv1-train (Fig. 8), rcv1-test (Fig. 9), url (Fig. 10) and kddb (Fig. 11), which are omitted in the main text due to the space limitation.

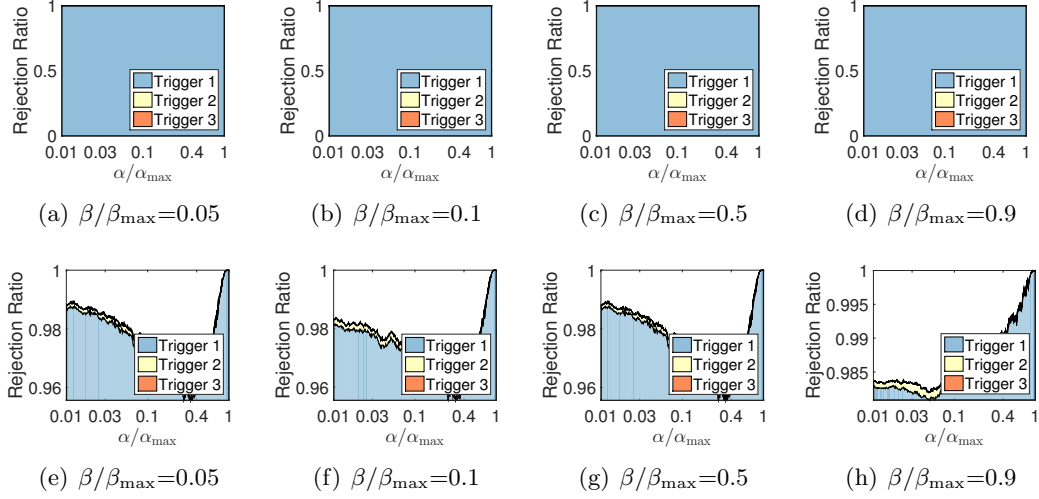


Figure 6: Rejection ratios of SIFS on syn1 (first row: Feature Screening, second row: Sample Screening).

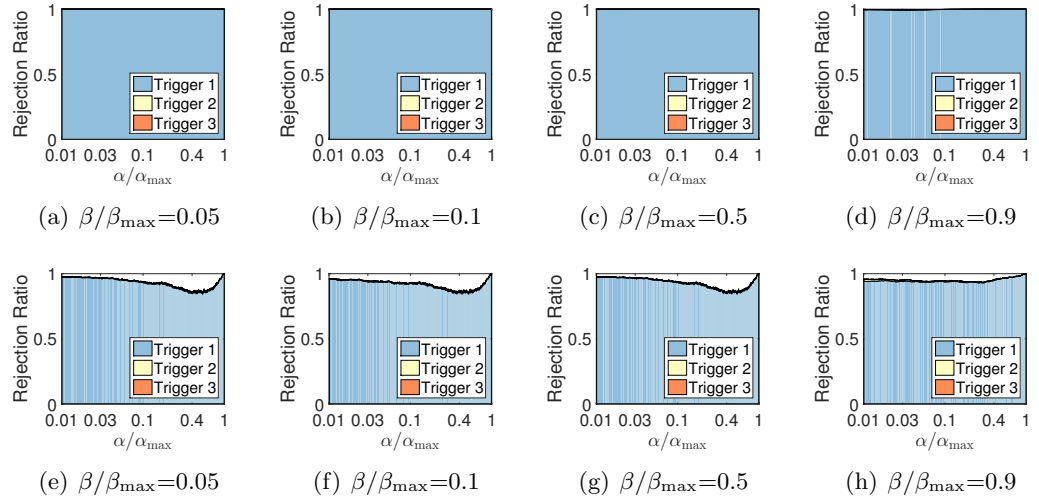


Figure 7: Rejection ratios of SIFS on syn3 (first row: Feature Screening, second row: Sample Screening).

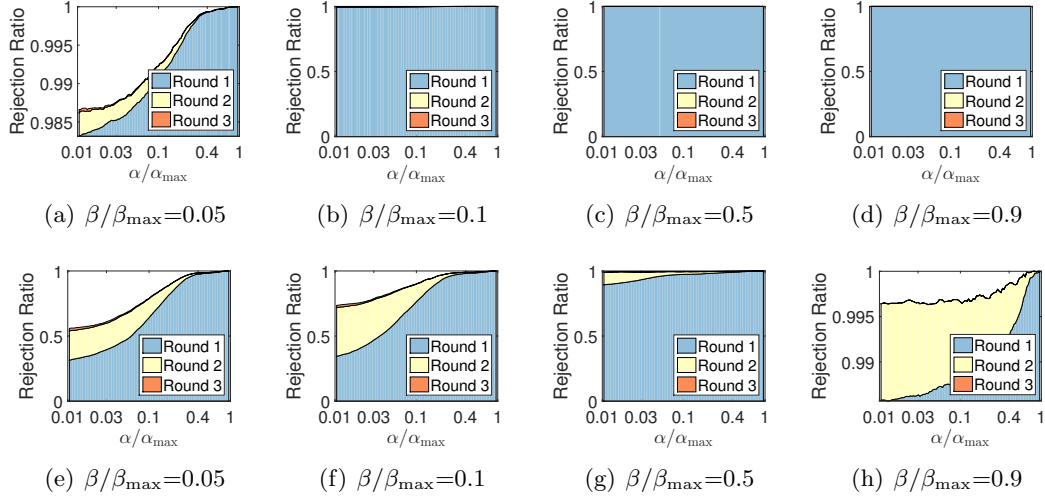


Figure 8: Rejection ratios of SIFS on rcv1-train dataset (first row: Feature Screening, second row: Sample Screening).

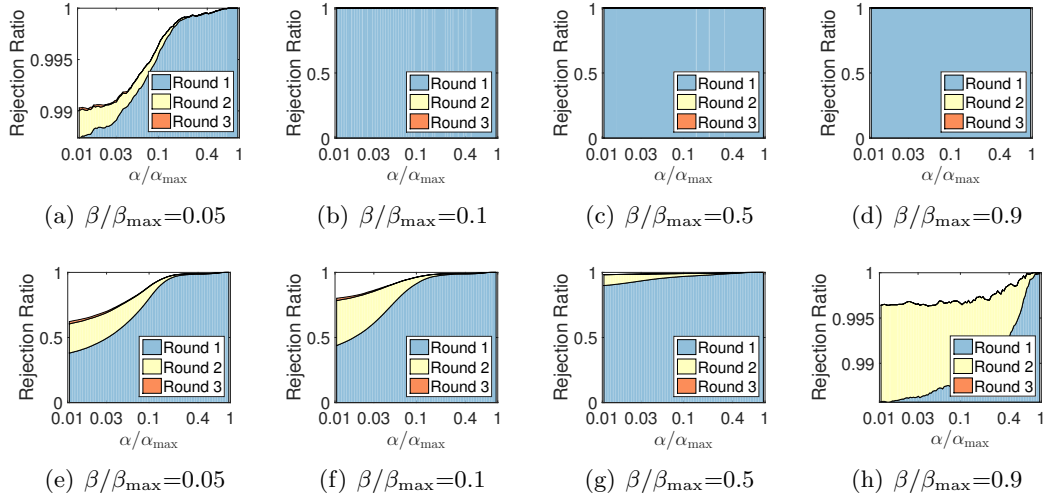


Figure 9: Rejection ratios of SIFS on rcv1-test dataset (first row: Feature Screening, second row: Sample Screening).

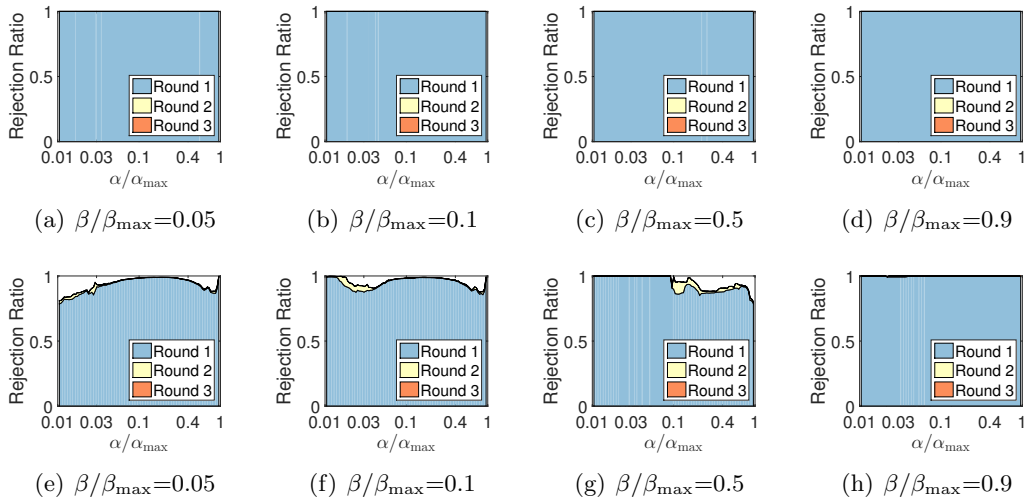


Figure 10: Rejection ratios of SIFS on url dataset (first row: Feature Screening, second row: Sample Screening).

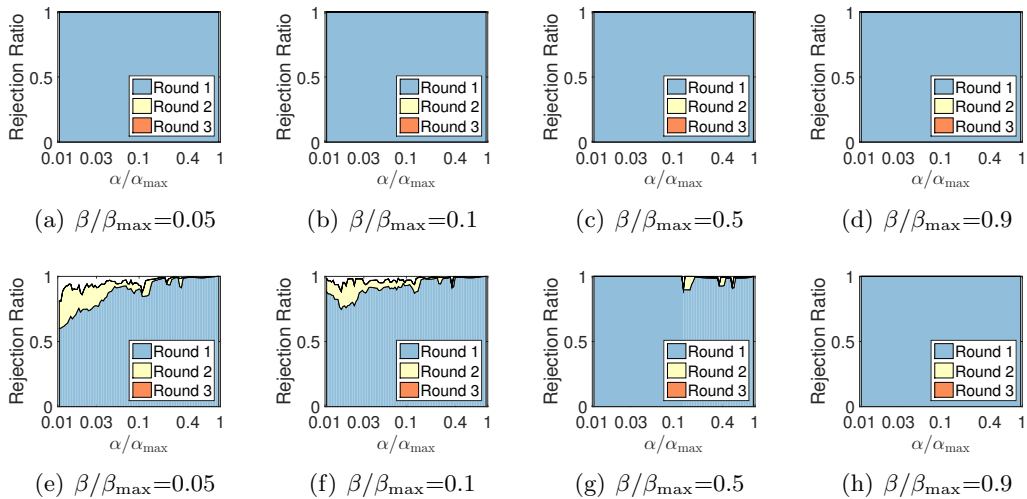


Figure 11: Rejection ratios of SIFS on kddb dataset (first row: Feature Screening, second row: Sample Screening).